,68
2/5/80

Lh. 645

LA-7885-MS, Vol. I

Informal Report

1-GWh Diurnal Load-Leveling Superconducting Magnetic Energy Storage System Reference Design

MASTER

University of California

LOS ALAMOS SCIENTIFIC LABORATORY

Post Office Box 1663 Los Alamos, New Mexico 87545

DISTRIBUTION OF THIS DOCUMENT IS UNLIMITED

1-GWh DIURNAL LOAD-LEVELING SUPERCONDUCTING MAGNETIC ENERGY STORAGE SYSTEM REFERENCE DESIGN

Compiled by

J. D. Rogers, W. V. Hassenzahl, and R. I. Schermer

Contributors

J. G. Bennett, H. J. Boenig, R. J. Bridwell, J. C. Bronson, D. B. Colyer, F. D. Ju, J. D. Rogers, and R. I. Schermer

ABSTRACT

A point reference design has been completed for a 1-GWh Superconducting Magnetic Energy Storage system. The system is for electric utility diurnal load-leveling but can also function to meet much faster power demands including dynamic stabilization. This study explores several concepts of design not previously considered in the same detail as treated here. Because the study is for a point design, optimization in all respects is not complete. This report examines aspects of the coil, the superconductor supported off of the dewar shell, the dewar shell, and its configuration and stresses, the underground excavation and construction for holding the superconducting coil and its dewar, the helium refrigeration system, the electrical converter system, the vacuum system, the guard coil, and the costs. This report is divided into two major portions. The first is a general treatment of the work and the second is seven detailed technical appendices issued as separate reports. The information presented on the aluminum stabilizer for the conductor, on the excavation, and on the converter is based upon industrial studies contracted for this work.

CHAPTER I

INTRODUCTION

A study has been undertaken to evaluate the magnitude in size, technical difficulty and detail, and cost of a 1-GWh Superconducting Magnetic Energy Storage (SMES) system for diurnal load-leveling for electric utility application. A 1-GWh size was chosen as being sufficiently large to make extrapolation to a larger size reliable and, unto itself, to be a size for which there could be considerable demand. Extrapolation of cost per unit of energy stored is, to the first order, inversely proportional to the maximum energy stored to the one-third power. The approach, used in the design, is to explore some variations to already conceived details of a SMES unit. In particular, these details are related to the dewar structure and the support and design of the conductor. Before any commitment is made to these or other concepts, a careful comparison is needed. To aid the study and establish credibility in areas in which unusual expertise is required, industrial consultants were used to assess the nature of the converters, the underground excavation for locating the superconducting storage coil, and high-purity aluminum to establish both methodology and costs. A brief discussion of the role of a large SMES unit in the electric utility industry follows.

The US electrical utility industry yearly transmits power to its customers at a rate equivalent to about 60% of its generating capacity. Aside from some downtime necessary for plant maintenance and standby equipment for emergencies, the average unused 40% of capacity represents unused capital investment. This situation arises because the demand for power varies periodically on a daily, weekly, and seasonal basis and randomly during periods of seconds to tens of minutes. Load variations on a yearly basis may differ by a factor of 2 or more.

The varying load is met through a combination of several power sources. The base load, which is about 45% of the peak power, is furnished by the more efficient fossil-fueled or nuclear generators that operate nearly 100% of the time at full capacity. The intermediate load, which is between 45% and about 85% of peak power, is supplied by less efficient plants cycled in and out of service; and the peak loads are met by gas turbines or diesel engines.

The base load plants may supply about 70% of the total system energy at the lowest delivered cost, whereas the intermediate cycling plants will furnish about 25% at significantly higher cost. The remaining 5% is derived from the peaking units. Although these units are relatively inexpensive in terms of

peaking units. Although these units are relatively inexpensive in terms of capital investment, they require costly and scarce fuels, such as JP-4 or Number 2 fuel oils; operate at low thermal efficiencies; and have high maintenance costs.

Electric energy usage is planned to increase about 45% by 1985. Thus, the industry must install about 200 000 MW of generating capacity at a total cost of $170 billion. However, if inexpensive energy storage were available today, part of this investment in generating capacity could be postponed. The potential savings associated with the utilization of energy storage systems are much greater than just those in the area of capital investments.[1] Ten percent of all generating capacity is presently in the form of gas turbines, and 2% of the total electrical energy used in the US is generated by these units. About 140 million barrels of Number 2 fuel oil would be consumed each year by these devices on utility systems by 1985. Because the possibility exists for energy storage systems to replace about 50% of the gas turbine capacity, the potential savings would be 70 million barrels of oil per year. Some other fuel such as coal or uranium would have to be consumed to generate the electrical energy that is to be stored.

One advantage of SMES over most other energy storage systems is its inherent high efficiency. Because there is no conversion of electrical energy to electrochemical, thermal, or potential energy, there are no losses associated with a conversion process. The expected efficiency is between 80 to 95% depending on the design, the size of the installation, and the mode of operation. The main losses are thermal losses, 2.6%, in the electrical interface between the utility system and the superconducting storage coil and electrical energy required to operate the refrigeration system to maintain the coil at a temperature of 1.8 K (2.4% for very large systems at 10 000 MWh, to about 15% for small systems at 10 MWh). Because the efficiency is great, there will be additional savings in fuel in the primary energy source, which will be in tons of coal or pounds of uranium. The total anticipated annual savings, if SMES systems were used today to replace 20% of all the non-baseload, oil-fired generating capacity, would be 40 million barrels of oil and, relative to the use of pumped-hydro, about 48 000 billion BTU savings in energy.

A SMES unit is built around two major components. These are the storage unit that is a superconducting coil and an electrical converter to operate and transform the current between the ac transmission line and the dc coil. All

other items in the system are ancillary to these two. A SMES system is shown in Fig. I-1.

Several aspects of a large SMES unit determined by earlier work are retained as features of this reference design. These include the operation of the superconductor in a 1.8 K 1-atm superfluid helium bath to reduce the cost of superconductor, the contoured, modular cold- and warm-wall helium dewar to accommodate thermal expansion and reduce material thickness, the location of the storage coil underground to reduce coil support construction costs, and a simple solenoid with a height-to-diameter ratio of about one-third. Some of these aspects should be evaluated further to assure that no viable alternatives exist.

Table I-I gives some of the parameters of the storage system. The technology base of this reference design and, hence, the parameters are considered to be within the state of the art. No discoveries or unusual inventions are needed to design and construct such a SMES system. At the same time, technology development is needed to establish construction methods that

TABLE I-I

1-GWh SMES SYSTEM PARAMETERS

Energy exchanged	3.6×10^{12} J (1.0 GWh)
Maximum energy stored	3.96×10^{12} J (1.10 GWh)
Coil diameter	132 m
Coil height	44 m
Coil thickness	20 cm
Tunnel width	3.0 m
Coil inductance	3170 H
Maximum current	50 kA
Minimum current	15 kA
Maximum field	4.5 T
Temperature	1.85 K
Minimum voltage	5.0 kV
Maximum voltage	16.7 kV
Maximum power	250 MW

will be reliable. Also, improvements in the technology base could alter the economics of such a major capital project.

REFERENCE

1. F. R. Kahlhammer, "Energy Storage: Applications, Benefits and Candidate Technologies," Proc. Symp. Energy Storage Electrochemical Society, March 1976 (Dallas, TX, 1976) pp. 1-20.

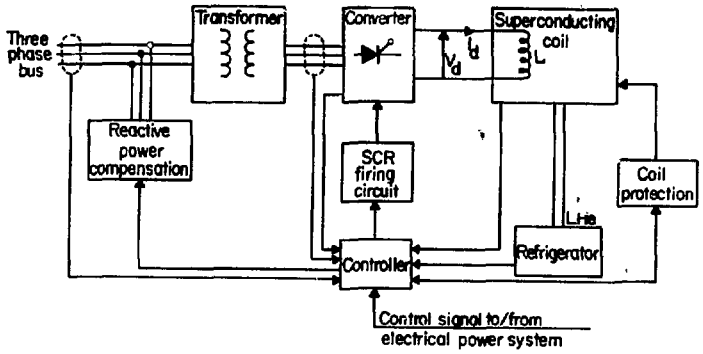

Fig. I-1.
Components of a superconducting magnetic energy storage system.

CHAPTER II
ENERGY STORAGE COIL AND CONDUCTOR

A. INTRODUCTION

At the heart of a SMES unit is the conductor, which carries the current that establishes the magnetic field where energy is stored. The conductor itself consists of two functional parts: (1) the superconductor, in which all the current flows under normal operating conditions, and (2) the stabilizer, which forms a parallel path of normal conductor where the current can flow in an abnormal, transient condition when a length of superconductor becomes resistive. The proposed conductor is a 50-kA superconducting cable sandwiched between two parallel stabilizing elements, which consist of high-purity aluminum jacketed with cold worked copper. See Fig. II-1. The interaction of current and magnetic field creates a transverse force on the conductor, which therefore must be located in a coil structure that transmits these forces to external supports. This chapter presents a conceptual description of the coil and conductor. Detailed design is discussed in Appendix A,[1] and the external supports are discussed in Chapter III and Appendix C.[2]

B. COIL PARAMETERS

The energy to be exchanged with the electric utility system is specified as 1 GWh, but the actual energy stored in the magnetic field when the coil is fully charged is not specified as the coil will not be fully discharged at the bottom of a daily cycle. Further, there are numerous choices for coil shape, dimensions, maximum field, coil winding pattern, and operating current that will give the same stored energy. The options are discussed in Appendix A and the characteristics are given in Table II-I. Note that the turns density decreases from the coil midplane toward the ends, as detailed in Table A-I.[1]

Many of these choices were made on the basis of generalized optimization studies that did not take into account any of the very expensive details that have been encountered in the course of the present study and that used different unit material costs from those used here. It is thus possible that this point design is not optimum.

TABLE II-I

1-GWh COIL CHARACTERISTICS

Stored energy	3.96×10^{12} J (1.1 GWh)
Energy exchanged	3.6×10^{12} J (1.0 GWh)
Average radius	66 m
Height	44 m
Radial thickness	0.20 m
Inductance	3170 H
Operating current at full charge	50 kA
Cryogenic coolant	Helium at 1.8 K, 1 atm
Number of turns	4280
Number of radial turns	5
Winding pattern	pancake
Radial turn spacing	0.60 cm
Axial turn spacing, midplane	2.69 cm
Axial turn spacing, end	11.7 cm

C. CONDUCTOR DESCRIPTION

The superconductor is multifilament NbTi, extruded in copper with a copper-to-NbTi ratio of 1.33, drawn to a 0.147-cm-diam strand, and formed into a 23-strand flat, transposed cable, 0.277 by 1.67 cm (Table A-II).[1] One advantage of this conductor is that its cost can be accurately defined, and it is within the ability of the superconducting wire industry to produce this cable. The cable can be formed in long lengths by cold welding the individual strands at well-spaced locations, and the amount of superconductor at any location can be adjusted or graded to the minimum amount necessary so that 50 kA always represents 90% of critical current in the local magnetic field. Grading is accomplished most safely by fabricating strands with a number of different copper-to-superconductor ratios.

Current density in the aluminum stabilizer is set at 15 kA/cm^2 by the requirement that for external protective action, 1% of the stored energy can be removed with a turn-to-turn potential of 100 V and a temperature rise in the aluminum of 100 K. The rather arbitrary figure of 1% corresponds to dividing the magnet electrically into roughly 10 segments. With this protection requirement, it is still possible to use an all-copper conductor. A less

stringent requirement allows the current density to be raised, which creates a stability problem for an all-copper stabilizer that is ameliorated by using a lower resistivity aluminum conductor.

This stabilizer design has several advantages. First, the length and mass required for a pancake are small enough so that the entire conductor for one pancake can be shipped to the SMES site in finished form. Second, although not assumed here, the shape and size of the stabilizer can be varied with position to minimize cost. This variation is possible principally because there is a larger conductor surface area exposed to coolant in the less-stressed regions of the coil.

Energy removal by the superfluid helium bath can be limited either by the maximum heat flux across the conductor-helium interface or by the maximum heat flux which can be transported along the interturn channels. The channels are designed large enough so that the surface heat flux of 5 W/cm^2 is limiting. The assumption is made that one-half of the conductor surface is occluded by support structure. The conductor is designed to be fully stable, so that when all the current is in the stabilizer, the heat generation is equal to the heat that can be carried away by the helium in contact with the exposed surface. A study has been performed by the Aluminum Company of America (ALCOA) on the cost of high-purity aluminum as a function of purity, based on the use of a proprietary process that they developed. This study is presented in Appendix B.[3] The cost of copper is taken as $1.50/kg.

Airco Superconductors, Inc. fabricated short lengths of copper-jacketed, high-purity aluminum stabilizer by a series of drawing and rolling operations. They produced samples with 20% copper by volume, with the copper in the full-hard condition and the aluminum with a residual resistance ratio >1000. The cost of producing large quantities of this material is unknown, but the assumption is that the fabrication cost is equal to the material cost. The actual cost of winding the coil is estimated in Appendix A.[1]

D. LOSSES

Under dc conditions, current will flow in a superconductor in a perfectly loss-free fashion. When the magnetic field is varied, as when the coil is charged and discharged in its daily cycle, the electric fields produce eddy currents that in turn produce power losses that must be removed by the liquid helium. The loss is calculated as the sum of several components. The only

nonnegligible contribution is the hysteretic loss due to eddy currents that circulate entirely within the superconducting filaments. An additional loss mechanism is due to the joints between coil pancakes, which are slightly resistive. The time averaged losses (Table A-V)[1] total 131 W with the coil holding full charge and 12 W with the coil holding minimum charge. Both of these losses are entirely due to joints, whereas losses while the coil is either being charged or discharged are 303 W.

Eddy current loss in the support structure depends upon the rate of change of the magnetic flux in the structure. This loss is negligible unless the structure forms a conducting ring with a radius of the order of the coil radius, in which case the losses are intolerable. The helium vessels must, therefore, contain an electrically insulating joint at one point along the circumference. This joint has not yet been designed.

Los Alamos Scientific Laboratory (LASL) experiments show that losses because of mechanical hysteresis should be negligible when the structural elements are cyclically stressed within the elastic region. These tests should be extended to cover additional materials and initial mechanical treatments. A potentially more important loss, whose magnitude is unknown, results from friction at the various interfaces within the structure. This loss needs to be carefully studied and controlled.

E. CONSTRUCTION

The radial and axial forces on the individual conductors are transmitted through the conductor stack to the helium vessel and then to the support struts. Whereas the accumulated radial load is small, the accumulated axial load may become very large. The transverse load-bearing limit is set by the allowable strain in the aluminum stabilizer. With a strain limit of 10^{-3}, the maximum load is 84 MPA (12.2 ksi). The helium vessel has already been divided into 13 separate sections, but the load within each section still accumulates to a large value. It is, therefore, proposed that the conductor stack within each section be divided vertically into two sections. The half nearest the coil midplane bears on the vessel end, while the half away from the midplane bears on ledges fitted to the inner and outer helium vessel walls as shown in Fig. II-2.

The vertical faces of the conductor must be supported lest they bulge outwards under the axial load. The conductors support one another through the radial spacers, which cover one-half the vertical conductor surface, while the outer wall of the helium vessel supports the outer conductor turn. A separate support band, of the same size as the conductor, supports the inner conductor turn. The radial spacers and support bands, which are made of aluminum alloy covered with electrical insulation, help support the accumulated axial load and are under a maximum stress of 73 MPA (11 ksi).

Material costs are taken as $2.50/kg for either aluminum alloy or stainless steel; and the fabrication and insulation costs are taken as twice this amount. Placement costs are included in the coil winding estimate.

F. COSTS

Aggregate costs of the various elements discussed in this chapter are given in Table II-II, and a more detailed breakdown and discussion is given in Appendix A.[1] The largest single item is the superconducting cable, which has a well-defined cost. There should be, however, a considerable margin for decrease in this price. The 1-GWh coil requires 10 years' output of NbTi at current production rates and a mass of cable 30 times that of the largest single order placed so far. Large scale production facilities should reduce costs.

TABLE II-II

COSTS FOR CONDUCTOR AND COIL

Item	Cost, 10^6
50-kA, graded and fabricated superconducting cable	43.2
Copper jacketed, aluminum stabilizer; materials	7.3
fabrication	7.3
Supports and spacers; material	6.2
fabrication	6.2
Coil winding labor	2.7
Total	72.9

REFERENCES

1. R. I. Schermer, "1-GWh Diurnal Load-Leveling Superconducting Magnetic Energy Storage System Reference Design; Appendix A: Energy Storage Coil and Superconductor," Los Alamos Scientific Laboratory report LA-7885-MS, Vol. II (1979).

2. J. G. Bennett and F. D. Ju, "1-GWh Diurnal Load-Leveling Superconducting Magnetic Energy Storage System Reference Design; Appendix C: Dewar and Structural Support," Los Alamos Scientific Laboratory report LA-7885-MS, Vol. IV (1979).

3. C. N. Cochran, R. K. Dawless, and J. B. Whitchurch, "1-GWh Diurnal Load-Leveling Superconducting Magnetic Energy Storage System Reference Design; Appendix B: Cost Study, High-Purity Aluminum Production," Los Alamos Scientific Laboratory report LA-7885-MS, Vol. III (1979).

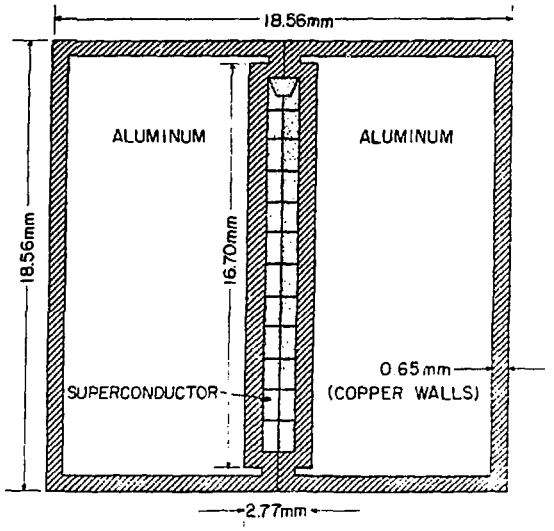

Fig. II-1.
Cross section of a conductor array, showing geometrical variable.

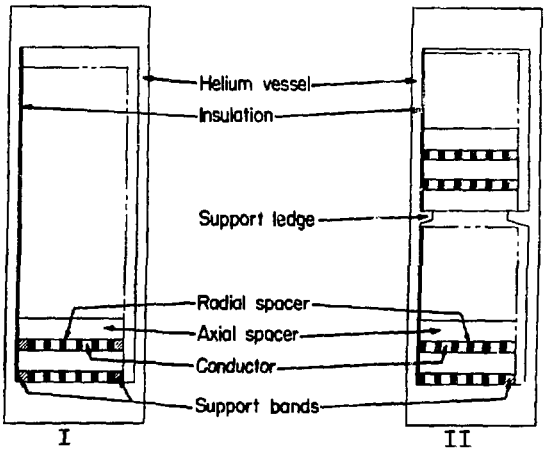

Fig. II-2.
Conductor support option. In option I, shown on the left, the axial load accumulates to the bottom of the helium vessel. In option II, pictured on the right, half of the axial load is taken by the ledges.

CHAPTER III
DEWAR AND STRUCTURAL SUPPORT

A. INTRODUCTION

Conceptual structura' design studies for the 1-GWh SMES system have focused on those components that are considered to be the most costly in terms of material and construction. The system can be built to this design with existing or easily developed technology and materials. A reference point on a cost hypersurface has been established by this design, and the many possible tradeoffs can move that point toward an optimal design. Several examples of cost savings are cited in Appendix C.[1] Tradeoffs that may optimize one area, such as minimal material cost, must be balanced against possible increased construction cost or a development that may accompany an alternative design. In short, though it is not clear that this design is the best design for cost, it is doubtful that unusually large savings will be realized in any alternative design.

B. GENERAL DESCRIPTION

The dimensions for the 1-GWh excavation cross section are shown in Fig. III-1. The excavation is made to house a large underground vacuum vessel. Inside this vacuum vessel are the inner vessels that serve as structural support for and contain the superconducting coil. The upper and lower ends of the outer vacuum vessel are sealed by means of an aluminum 5083 bellows that joins to an end seal structure. The upper end seal structure will have the necessary penetrations for construction purposes and piping. Personnel access to the tunnel will be through the radial access drift tunnel.

The inner helium vessel is segmented into 13 sections with numbers 1 through 6 above and 7 through 12 below the central segment. The central segment is numbered 13. The helium vessel is a rippled structure in the plan view. See Section AA of Fig. III-2. Support struts, located every 2 m on centers circumferentially, transmit the radial and axial magnetic forces to the outer wall of the excavation. The general concept is based upon struts proposed by the University of Wisconsin.[2] The struts have been divided axially into an 18.2-m central section, in which the axial loads are very small, plus two 12.9-m end sections in which the axial loads are greater than the radial loads.

C. OUTER VACUUM VESSEL

The vacuum vessel is to be constructed of aluminum 5083 in the H-38 condition. The vessel will be a continuous shell except for required penetrations for piping, conductors, and access. This shell will be constructed from seam-welded aluminum plate, 2.5 mm thick. The shell will be supported by 0.3-m long rock anchor supports on a 1- by 1-m spacing pattern. The rock-anchor-to-shell joint will be designed as a vacuum tight welded joint. The vessel material thickness near the high-stress region of the joint will increase to 17.0 mm to accommodate potential annealing of the aluminum during welding. The plates will be seam welded in the center of the support pattern. The rock-anchor supports will be 2.48-cm-diam aluminum and will anchor the liner to the shot-creted walls of the tunnel. The support pattern on the external wall will be planned not to interfere with the copper rock-heating pipes, which are also on 1-m centers. A bellows seal will join the vacuum vessel walls at all large penetrations and at the top and bottom of the tunnel. Construction of the shell will begin as soon as completion and curing of the shot crete allows. The welds will be subjected to vacuum testing as construction proceeds.

The material for the vacuum vessel and bellows is expected to cost $245 000 and $123 000, respectively. The design considerations for the vessel walls are given in Appendix C.[1]

D. LOW-THERMAL CONDUCTIVITY SUPPORT STRUTS

Construction of the low-thermal conductivity support struts on the outer wall will follow behind the vacuum liner. The struts will be constructed from the top downwards on 2-m centers circumferentially. The strut components and materials are shown in Fig. III-3. Construction will proceed piece by piece away from the outer tunnel wall and end at the extruded dewar support weld plate. All connections are bolted through friction connections with SAE Grade 8 38-mm bolts. All bolts are torqued to 6.5 kN-m.

The design of the strut is discussed in the Appendix C.[1] Figure III-4 shows the strut cross section and specifies the various thicknesses that are used in Tables III-I and III-II. Table III-II gives material volume and costs for the support struts.

TABLE III-I

DIMENSIONS OF SUPPORTS

Notation (Fig. III-4)	Center Strut, m	End Struts, m
L1	0.435	0.435
L2	0.480	0.480
L3	0.535	0.535
T1	0.014	0.068
T2	0.015	0.069
T3	0.032	0.16
r	0.20	0.20
t_1	0.14	0.14
t_2	0.03	0.03
Length	18.2	12.9

TABLE III-II

3-SECTION SUPPORT STRUT MATERIAL COSTS

Segment Numbers	G-10 Volume m^3	Estimated Stainless Steel Weld Plate Structure Volume m^3	Stainless Steel Connection Plate Volume m^3	Bearing Plate Volume m^3	No. of 38-mm High Strength SAE Grade 8 Bolts	Total Steel Volume m^3	G-10CR[b] Costs at $8/kg 10^3	Total Stainless Steel Costs 10^3	Total Fastener Costs[a] 10^3	Single Strut Cost 10^3	*Total* Segment Costs 104 Struts Circumference 10^6
1-6	2.02	0.52	0.433	0.16	592	1.11	32.4	19.3	11.8	63.5	6.6
13	0.58	0.73	0.612	0.23	406	1.57	9.3	27.2	8.3	44.8	4.7
7-12	2.02	0.52	0.433	0.16	592	1.11	32.4	19.3	11.8	63.5	6.6
										Total	17.9

[a]Fastener costs assumed to include all lengths of bolts plus nuts and washers at an average cost of $20/fastener.

[b]Density for high glass content taken as 2 g/cm^3.

E. HELIUM VESSEL

The 13 helium vessels are designed to provide for helium containment and to transmit the loads from the conductors to the supports. A portion of the rippled geometry of the vessel is shown in Fig. III-5 with geometric variables identified. Figure III-6 shows the vessel cross section and the rest of the variables used in the Table III-III headings. Table III-III gives the material volumes and costs for the 13 helium vessels.

The helium vessel material is A304-LN austenitic stainless steel. The width, W, of all dewars is 0.2 m. Construction of these vessels can follow the completion of two adjacent support strut sections and proceed inward away from the support strut. The helium-vessel outer wall, Figs. III-4 and III-5, will be welded to the support weld plate, followed by the end closures. At this time crews will construct the coil, cooling pipes, and other structure required on the interior of the vessel. The helium-vessel inner wall, Fig. III-6, will be built following completion of the construction internal to the dewar. All welding is to be leak-checked. When the inner vessel wall of Fig. III-6 is welded, the construction of the structure will essentially be complete. Appendix C[1] presents design considerations for the helium vessel.

TABLE III-III

A304-LN STAINLESS STEEL 13-SEGMENT HELIUM VESSEL

SEGMENT NUMBERS	RADIAL DESIGN PRESSURE (MPa)	Vessel Geometry[a]							Single Segment Volume of Material (m^3)	Costs	
		R (m)	Ω (m)	H (m)	ϕ (deg)	h_i (cm)	h_t (cm)	h_s (cm)		Single Segment $10^6	Total $10^6
1 and 7	2.5	1.21	0.2	2.2	45	1.0	2.0	1.6	27.6	0.48	0.96
2 and 8	3.7			1.7			9.2	3.4	39.2	0.68	1.36
3 and 9	4.0			1.8			7.2	3.1	37.3	0.65	1.30
4 and 10	4.7			2.0			5.2	2.8	37.9	0.66	1.31
5 and 11	5.4			2.3			3.8	2.5	39.7	0.69	1.37
6 and 12	5.5			2.9			2.4	2.0	42.0	0.73	1.45
13	5.7			18.2			1.0	1.4	203.7	3.52	3.52
										Total	11.3

[a]Dimensions are defined in Figs. III-5 and III-6.

F. SYSTEM COST

The installed costs of this system and the per unit materials costs are given in Table III-IV. A factor of 3 times the computed material cost has been used to determine the installed cost. This factor may be somewhat high and its effect is discussed in Chapter IX below.

G. DISCUSSION

Potential savings in material cost can be investigated through design changes in some areas. The overall costs cannot be drastically affected without major design philosophy changes. Three such major changes are evident. In the first, stainless steel is considered for the dewar structural material because of the available technology for welding thick sections for reliable vacuum tight joints, etc. If similar technology for very thick aluminum sections can be made available, there would be potentially large material cost savings.

TABLE III-IV

IN-PLACE COST FOR 1-GWh SMES STRUCTURAL COMPONENTS

Component	Cost, 10^6
Vacuum walls	0.74
Vacuum-wall anchor system	1.54
Bellows seals, upper and lower enclosure structures	0.68
Low-conductivity support struts	53.7
Helium vessels	33.9
Total	90.56

Material Costs

Aluminum	$\$4880/m^3$ ($0.80/lb)
G-10 CR	$8/kg
A304 stainless	$\$17300/m^3$ ($1.00/lb)

The second most promising concept is the wire rope conductor design discussed in Appendix C.[1] Such a self-supporting conductor design would be a highly efficient structure and would eliminate the dewar as a load-carrying member. There may also be electrical advantages, such as being able to isolate a single turn by means of selective switching. This concept should be investigated further.

The third possibility is to use considerably less expensive oriented fiber-reinforced polyester or other reinforced support structure material rather than the G10CR fiber glass reinforced epoxy.

REFERENCES

1. J. G. Bennett and F. D. Ju, "1-GWh Diurnal Load-Leveling Superconducting Magnetic Energy Storage System Reference Design; Appendix C: Dewar and Structural Support," Los Alamos Scientific Laboratory report LA-7885-MS, Vol. IV (1979).

2. R. W. Boom, ed., "Wisconsin Superconductive Energy Storage Project," Vol. I and II, Engineering Experiment Station, College of Engineering, University of Wisconsin, Madison, WI (1974 and 1976).

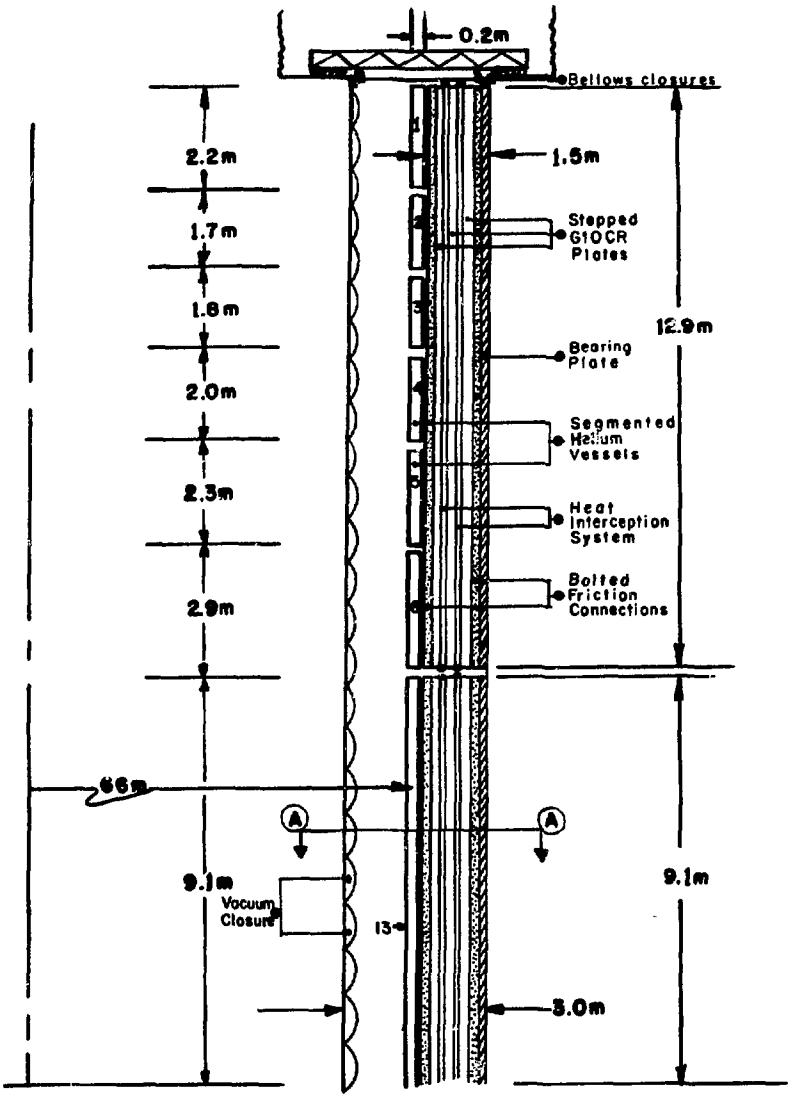

Fig. III-1.
Dimensions and cross section of the
13-segment dewar concept.

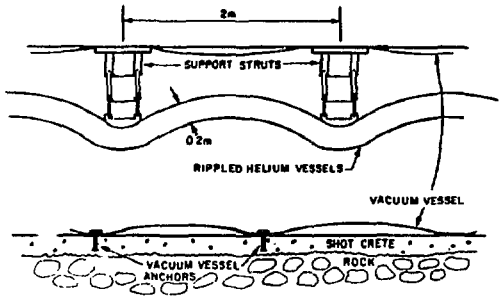

Fig. III-2.
Plan view of Fig. III-1 showing rippled dewar concept, section AA.

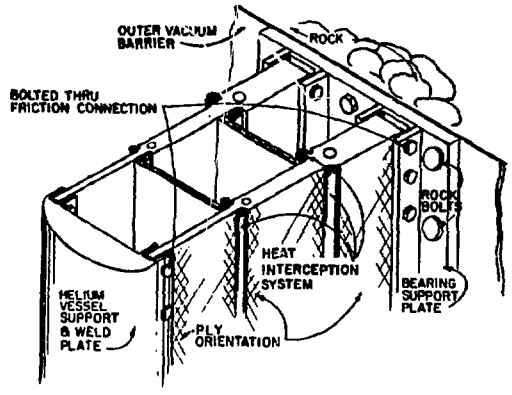

Fig. III-3.
Low-thermal conductivity support components.

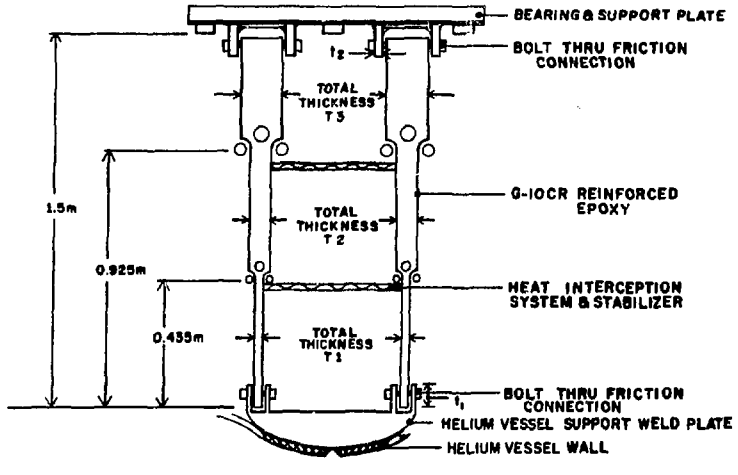

Fig. III-4.
Cross section of support.

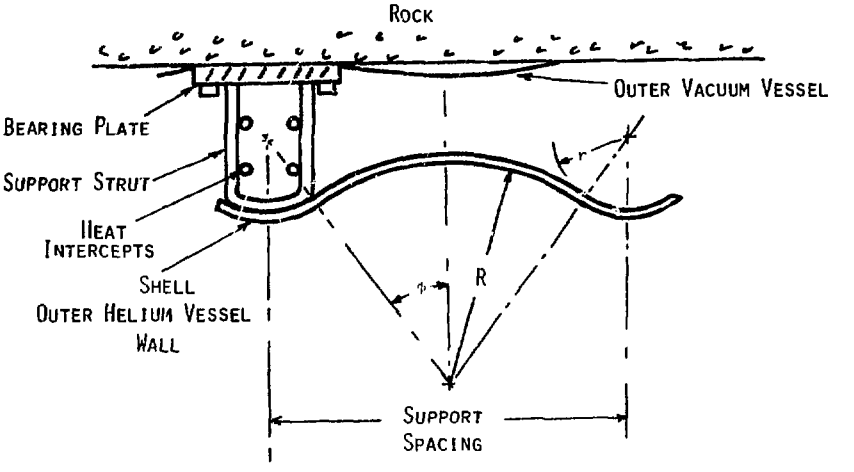

Fig. III-5.
Schematic of rippled-dewar geometry identifying the variables r, R, and ϕ.

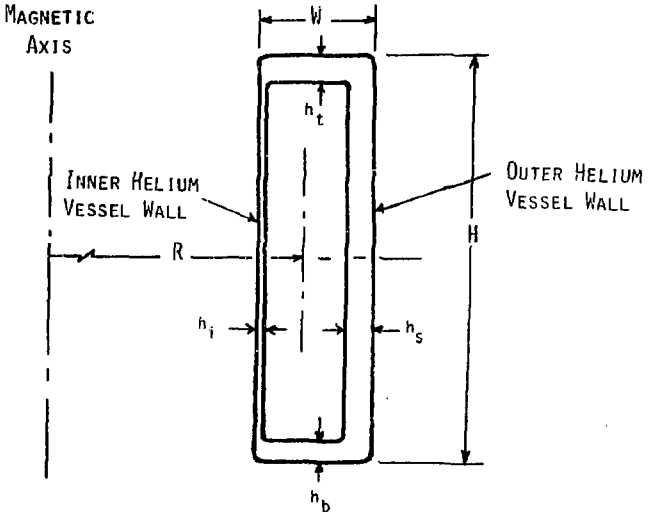

Fig. III-6.
Cross section of helium vessel identifying notation for dimensions of Table III-3.

CHAPTER IV
UNDERGROUND EXCAVATION

A. ROCK TUNNEL ANALYSES

SMES devices are planned for installation in underground tunnels. Structural supports from the cold inner helium dewar to the 300 K rock make use of the rock as an economical load-bearing material. The rock is under compression from its own weight and the earth's overburden. The magnetic forces simply reduce these built-in compressive stresses. Lorentz forces produced in the energy storage coil deform the rocks that form the tunnel walls. Elastic analyses of granite under the coil load distribution generate compressive stresses having maximum values of about 103 bars and shear stresses of about 17 bars in the surrounding granite. These values are about 10% or less of limiting strength criteria, so the tunnels should be stable. However, rock bolting is recommended just below and above the access rooms associated with the vertical coil-dewar tunnel because of stress enhancement in these regions.

Consideration of the effects of cyclic loading during the 30-yr history, the hydrologic conditions, or the locating of the dewar in weaker rocks suggests induced stresses may approach failure; and rock bolting for wall stabilization is a necessity.

The mechanical finite-element analyses described in this chapter deal with the superconducting coil housed in a 132-m-diam annular tunnel operating at a field of 4.5 T and a storage capacity of 1 GWh. The tunnel geometry is shown in Fig. IV-1. The calculation was done for the midplane located 207 m below the surface instead of 200 m. The effect of this change on the stresses is not significant.

Because this is a point reference design and the site has not been selected, the strength and behavior of all rock types which might house SMES have not been considered. Rock properties for isotropic granite were chosen for comparison with calculations of Fuh et al.[1] for a different tunnel design.

The tunnel for the 1-GWh reference design for the SMES system consists of an annular ring. This annular excavation contains the dewar and supports the cryogenic structure that contains the superconducting coil. The tunnel is vertical, 3 m wide and 44 m high, with dewar closure, machinery, and access rooms at the top and bottom. The rooms are 5 m high and 6 m wide. Because of

symmetry, only the portion of the tunnel above the midplane is shown in the figures and only one-half of the coils is discussed.

The analyses deal with the effects of the axial and radial Lorentz forces imposed on the outer tunnel wall. The first dewar segment is physically connected to the wall so the loads are taken more than 3.1 m away from the end access room. Segments two through six are attached for a distance of 12.9 m vertically along the tunnel wall. The axial pressure is transmitted to the wall as constant axial components equal to 108 bars (1580 psi). The radial load is a minimum at the top and bottom of the coil tunnel and is a maximum at the midplane of the tunnel. The effect is to increase incrementally the radial pressure from 12.5 bars (182 psi) to a peak value of 100.5 bars (1470 psi) along the entire outer tunnel surface. The total force from the field is resolved into radial and axial components. Figure IV-2 shows the resolved components.

Although the radial load components are everywhere outward, because of their low value at the upper and lower coil segment and when combined with the high axial loads on the end segments, the resultant average force on the rock wall is inward. This is shown for the upper segment in Fig. IV-2 with inward pointing arrows denoting a 12.5 bar average pressure. This effect arises because the moment, is dominated by the axial forces tending to roll the extreme portions of the end dewar segments toward the axis of the coil. The method of conductor and helium dewar support and their positions, which give rise to the moment, are presented in Chapters II and III. In a more complete engineering design, the local force distribution, which is available but was averaged for this analysis, will need to be considered in detail.

Site selection requires modeling many different rock types, such as granite, basalt, limestone, shale, etc. Granite was chosen for this point reference design. The rock properties for granite are assumed to have a Young's modulus of 500 kb (7.5×10^6 psi) and a Poisson's ratio of $\nu = 0.25$. The rock is modeled as an elastic, homogeneous, isotropic continuum. These assumptions allow comparisons of calculated stress levels with other rock properties from Clark[2] to determine the stability of the tunnel when subjected to the initial charging of the coil. Because of the paucity of information for long-term fatigue under cyclic loading, the effects of joints on the rocks, and the interaction of the hydrologic environment, the stability calculations are

biased toward instantaneous steady-state models. Long-term considerations will increase the probability of tunnel instability.

The maximum principal compressive stress is 103 bars (~1495 psi) occurring about 15 m below the top of the room as shown in Fig. IV-3. The minimum principal stress is compressive and is 75 bars (~1090 psi) as shown in Fig. IV-4. The negative notation on the figures denotes compressive stresses. The hoop stress is compressive with a maximum value of 26 bars (~380 psi) as shown in Fig. IV-5. Figure IV-6 shows the increasing shear stress approaching the midplane. The shear stress is quite low.

Rock stability criteria are usually based on uniaxial compressive strength measurements. For granite, the compressive strength[2] is about 2 to 4 kb. Tensile strength is generally related to compressive strength by the rule of thumb that $S_T = 0.1\ S_C$; therefore, the tensile strength would be in the range 0.2 to 0.4 kb. Shear strength is related to compressive strength by $S_s = 0.5\ S_c$, and the shear strength would have the range 1 to 2 kb. All stresses are well below these limits and the tunnel should be quite stable.

The preceding elastic models ignored cyclic loading of the coil for 30 yr, effects of joints in the rock and the hydrologic environment on rock strength, and ground motions because of nearby large earthquakes. Although data on these items are very sparse, limited research suggests that each contributes to a decrease of the stability criteria.

If another rock type such as dolomite, limestone, or shale is chosen for the tunnel site and is not as strong as granite, then the loads used here may violate stability criteria in these weaker rocks below the surface. Creep models should be used to evaluate the cyclic fatigue behavior of host rocks. Rock-mechanics studies are necessary to ascertain coefficients of strength for the creep constitutive laws. Related measurements of interactive effects of pore pressure and fracture are also needed. The uncertainties presented here should be resolved in any specific SMES tunnel construction. In the absence of their resolution, extensive rock bolting will be necessary.

The rock-mechanics analyses were performed for the storage coil at depths of 200, 300, and 500 m to determine the minimum depth where only miminal compressive stresses still exist in the rock structure subjected to the maximum loads resulting from a fully charged coil. To locate the coil at any depth, about 200 m would decrease the compressive stresses to undesirably low values

with the risk of developing tensile stresses. Only the 200-m depth results are presented here.

B. TUNNEL EXCAVATION AND CONSTRUCTION COST STUDY

A consulting contract was placed with Fenix and Scisson, Inc., a mining engineering firm, to make a SMES tunnel excavation, construction, and cost study. The tunnel conforms to the configuration of Fig. IV-1. The study considered locating the coil at depths of 200, 300, and 400 m. Only the cost estimates for the 200-m depth are presented here.

The excavation study originally called for six 1.82-m-diam drill holes with steel linings for vacuum pump-out lines, a 3.96- by 3.35-m production shaft with concrete-lined stabilized walls and a ship hoist for assemblying the storage coil, a 3.7- by 3.7-m horizontal shaft extending 250 m horizontally from the center line of the tunnel axis to an equipment room at the 227-m level, and a 20- by 20- by 10-m-high equipment room with its own 3.9- by 3.9-m vertical service shaft. The rock walls throughout the excavation are to be stabilized with rock bolts.

The main storage coil tunnel is lined with impermeable load-bearing concrete walls with a minimum compressive strength of 422 to 563 kg/cm^2. Steel load-bearing plates are mechanically anchored to both walls with 50-mm-diam by 1-m-long zinc-plated rock bolts. The zinc plating is required for a 30-yr life. Twenty-five-millimeter copper pipes on 1-m centers are imbedded in the concrete lining of the tunnel walls. These supply heat to prevent freezing of the concrete and rock because of the heat leaks into the dewar. Provision was made to remove ground water seepage from behind the concrete. An underground equipment room provides a saving in the refrigerator system. Its remote location from the coil was necessary to have the equipment in a low fringe field of <200 G for maintenance.

Fenix and Scisson estimated the total cost of the above work at $48.5 million. Subsequent analysis and redesign resulted in a significant cost saving. The major design changes follow.

1. The relocation of the vacuum pumps in the underground equipment room makes the six drilled shafts unnecessary, provided the equipment room and the horizontal drift leading to it are somewhat enlarged. The saving is $9 million.

2. The vertical shaft to the equipment room can be eliminated and the main production shaft used for all mining and maintenance functions, provided the main shaft is relocated and the horizontal production drifts are extended. The saving is $0.7 million.

3. The excavation study was performed at a stage in the design when the axial magnetic forces were to be transmitted to both inner and outer tunnel walls. Under the final concept, in which load-bearing struts do not contact the inner wall, this wall need not have a thick concrete lining, of lower quality, and does not require heating pipes. The saving is $2.0 million.

4. The study included a steel bearing plate at the base of each support strut, at a cost for material and placement of $3 million. These plates have since been redesigned and their cost included in Table III-II, although the cost of the rock bolts which fasten these plates to the tunnel wall are still counted in the present chapter. These bolts, at $8 million, are a major cost item.

The adjusted cost for excavating and preparing the tunnel, after considering the savings of items 1 through 4, becomes $33.8 million.

REFERENCES

1. G. F. Fuh, T. Doe, and B. C. Haimson, "Design of Underground Tunnels for Superconductive Energy Storage," F. Wang, and G. Clark, Eds., Supplemental Volume, Eighteenth US Symposium on Rock Mechanics, US National Comm. Rock Mech., National Acad. Sci., (Colorado School of Mines Press, Boulder, CO, 5A5-6 1977).

2. S. P. Clark Jr., "Handbook of Physical Constants," Geol. Soc. Am. Mem. 97, 587 (1966).

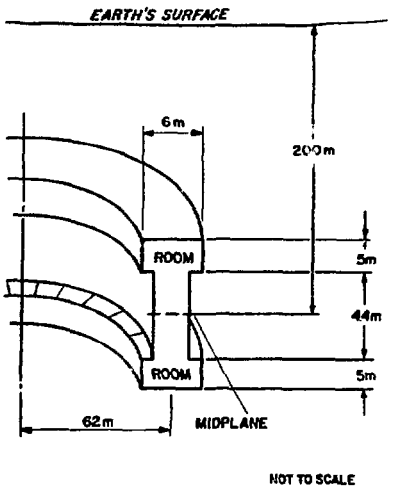

Fig. IV-1.
Schematic of quarter section of tunnel designed to contain SMES device.

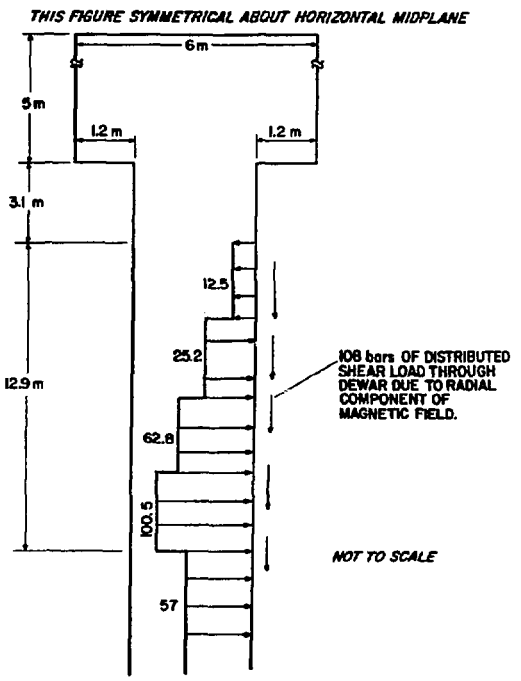

Fig. IV-2.
Loading system for 4.5-T unit with coil supported by outer tunnel wall.

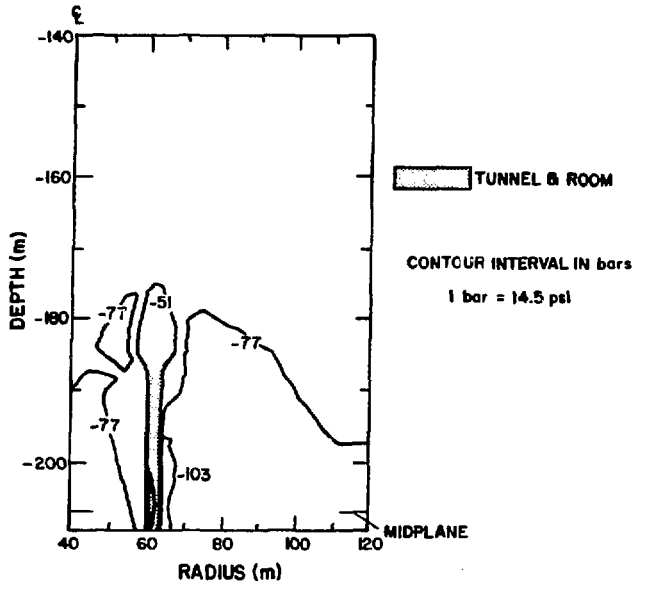

Fig. IV-3.
Maximum principal compressive stress with coil supported by outer tunnel wall.

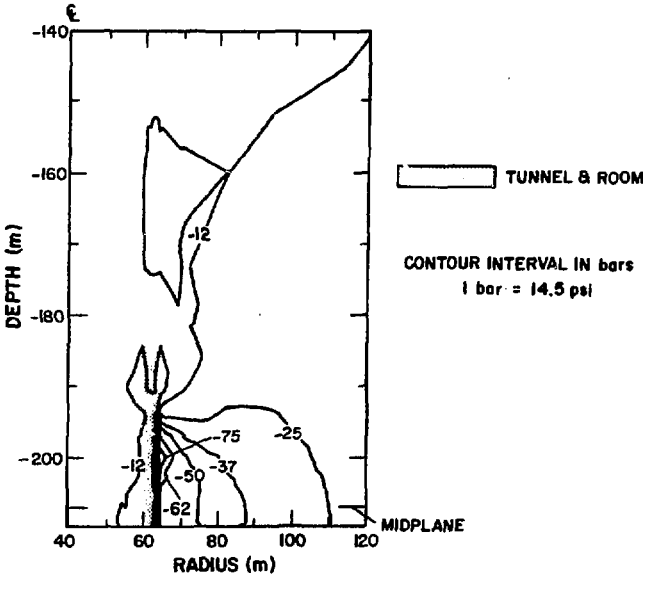

Fig. IV-4.
Minimum principal compressive stress with coil supported by outer tunnel wall.

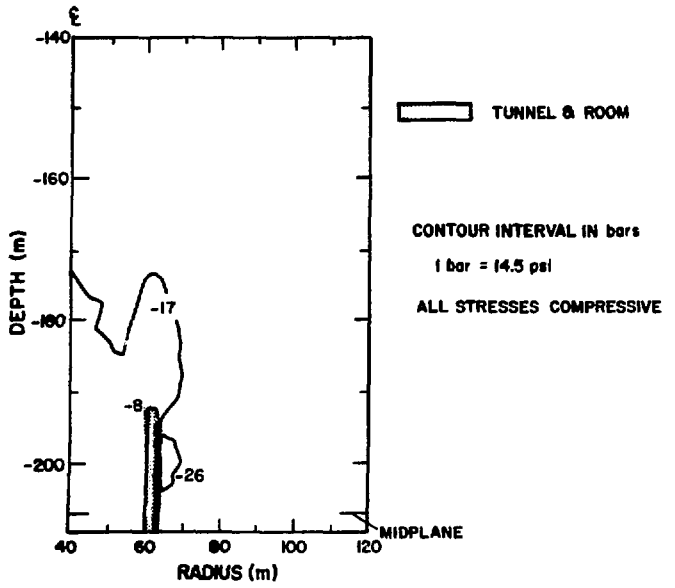

Fig. IV-5.
Hoop stress with coil supported by outer tunnel wall.

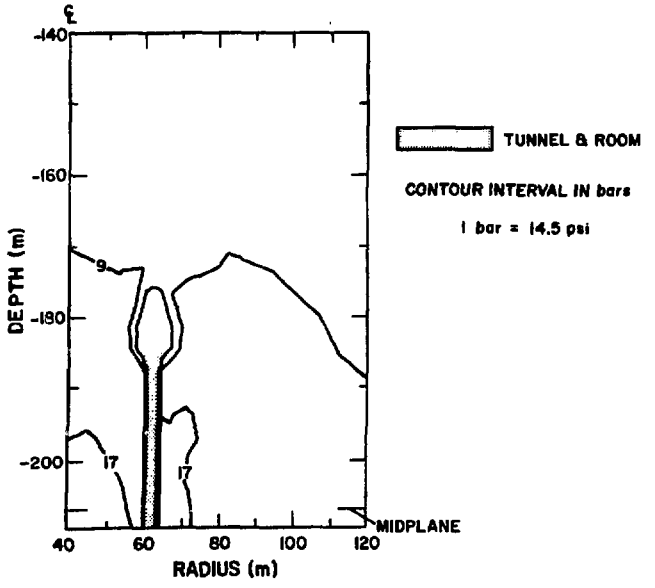

Fig. IV-6.
Maximum shear stress with coil supported by outer tunnel wall.

CHAPTER V
CRYOGENIC SYSTEM

A. INTRODUCTION

Cooling of the superconducting coil is accomplished by means of a two-fluid system. The coil is immersed in a superfluid bath at 1.8 K that is maintained with an overpressure of 1 atm. The 1.8 K temperature is achieved by two means. The first is a thermal barrier located in a small cross-sectional area of the dewar. This barrier sustains a temperature gradient with a small heat leak to an overlying layer of 4.5 K liquid helium. The 4.5 K liquid is then pressurized at about 1 atm with cold helium gas. The second device is merely a heat exchanger, a set of vertical pipes, located within the 1.8 K 1-atm liquid helium bath. This heat exchanger operates at 1.8 K and 12.5 torr on the refrigerant side. The largest heat load to be removed is that due to thermal conduction along the support struts. The refrigerator provides the liquid helium and cold gas to the system, which distributes liquid helium to cool the coil to 1.8 K and cold gas to cool the support struts and dewar radiation shield. The refrigerator consists of the helium compressors, cold box, low pressure pumps, and helium storage facility.

Helium gas is compressed and piped to the cold box where it is cooled by heat exchange and energy extraction. The resulting liquid helium is piped to the dewar at 4.5 K where it is expanded to 1.8 K and 12.5 torr (0.0165 atm) in the heat exchanger. 1.8 K superfluid helium on the low-pressure side of the heat exchanger absorbs heat from the bath of liquid helium surrounding the coil. Low-pressure vapor is returned to the cold box. Some of the 4.5 K liquid cools the power leads. The liquid is vaporized by the leads and returned to the helium compressor at approximately 300 K.

The support struts and dewar radiation shield are cooled with high-pressure helium gas from the cold box at 63 and 12 K. This 18.0-atm gas undergoes a 10.0 K temperature rise across the parts to be cooled and then is recirculated through the cold box. Low-pressure helium pumps provide the continuous pumping power to move 12.5-torr helium gas through the transfer lines and cold box for heat exchange and to raise the pressure to about 1.0 atm at 300 K to feed the main helium compressors.

With the dewar buried 200 m below the ground surface, the gravity head would represent a part of the 12.5-torr pressure drop available between the dewar and the pumps if they were located at the surface. Locating the pumps at the surface is more costly because of the additional pressure drop and because of the need for low-pressure transfer lines to and from the surface. Therefore, they are located underground in the equipment room with the cold box.

Equipment that will need routine servicing and maintenance must, for occupational reasons, be in a magnetic field of 200 G or less. Thus, the below-ground equipment room for the cold box and pumps must be 250 m from the center of the magnet. See Fig. V-1. All of the cryogenic transfer lines to and from the cold box and dewar are in a horizontal tunnel between the two. High-pressure helium supply gas from the compressors to the cold box and low-pressure return gas from the cold box and pumps to the compressors will be at about 300 K. These pipe lines will run in the vertical shaft between the compressors, which are at the surface, and the cold box and pumps below ground. Adjacent to the compressor will be a helium storage facility and a water cooling system consisting of either a cooling tower or cooling pond, to provide cooling water to the compressor, helium pumps, and vacuum pumps.

Liquid helium will be stored at 4.5 K on the surface in eight dewars during periods when the coil and coil dewar must be nonoperational for maintenance. A vertical transfer line runs in the equipment room service shaft to carry helium to the surface. A liquid-helium pump, located beneath the coil dewar, provides a 225-m head to transfer the liquid, in reverse direction, through the 4.5 K coil-dewar heat exchanger supply line and the vertical transfer line.

A comprehensive description of the cryogenic system is presented in Appendix E.[1] This appendix covers the major heat loads, the physical equipment with appropriate functional parameters, and costs. The major features that have been evaluated are system configuration, equipment location relative to the storage coil; heat loads from the power leads, structure, dewar, and coil; transfer lines; refrigerator including compressors and cold box; the 1.8 K dewar heat exchanger; helium inventory; cooling tower; and helium storage. This chapter summarizes Appendix E.[1]

B. HEAT LOADS

Heat loads are removed by the refrigerator in three different temperature regions.

1. Thermal conduction and Joule heating in the power leads evaporates helium at 4.5 K and returns 300 K gas to the cold box.

2. Heat conducted along the support struts and radiated from the dewar heat shield is removed by temperature stations at 63 and 12 K located on the support struts (Fig. III-3).

3. Heat conducted along the support struts, heat conducted between the 4.5 and 1.8 K 1-atm helium baths, heat radiated from the cold innermost shield, and heat generated in the coil are removed through the 1.8 K heat exchanger at 12.5 torr.

The power leads carry the 50-kA current through the dewar shells to the coil and generate Joule heating and some conduction losses that are removed by heat exchange to vaporized liquid helium. Coil losses are described in Chapter II and Appendix A[2] and arise from the diurnal current change associated with the energy charge-discharge cycle. The structural supports described in Chapter III and Appendix C[3] transmit the weight of the coil and helium vessel and the magnetic forces to the rock wall of the underground tunnel. Thermal conduction along the supports or struts is a heat load intercepted at 63, 12, and 1.8 K. Radiation to the dewar is intercepted by an intervening 63 K shield between the helium vessel at 1.8 K and the warm dewar vacuum jacket. The transfer lines are all radiation shielded and traced with 63 K helium gas. The

TABLE V-I

CRYOGENIC HEAT LOADS, kW

		Temperature Level, K		
	ℓ/hr	1.8	12.0	63
Power leads (4.5 K)	250			
Coil losses		0.30		
Support struts		1.44	9.3	127
Dewar radiation		0.50		16
Transfer lines				1
Total	250	2.24	9.3	144

heat loads from these sources are given in Table V-I. The totals of the first two columns convert to 4.1-kW refrigeration required at 4.5 K.

C. TRANSFER LINES

The transfer lines are double-concentric vacuum-jacketed lines, one each between the cold box and the dewar, for each of the three thermal levels of refrigerant at 4.5, 12, and 63 K. The 4.5 and 12 K lines are shielded and traced with 63 K gas. A fourth transfer line runs to eight liquid helium storage dewars at the surface above the equipment room. Fluid from the cold box to the dewar is through the center tubes of the lines and is returned to the cold box through the annular space of the concentric tubes. This concentric transfer line doubles as a heat exchanger between 1.8 K vapor from the dewar and acts as a coolant for the 4.5 K liquid flowing to the dewar. The 1.8 K vapor into the vapor return line is warmed to nearly 4.5 K at the exit of the return line; hence, the transfer line is labeled as a 4.5 K vapor return line. Tube dimensions are given as effective hydraulic diameters. The transfer line parameters are given in Table V-II. The $5.04 million total cost should be increased by 100% for valves and 50% for installation for a final total cost of $12.6 million.

TABLE V-II

TRANSFER LINE PARAMETERS

	4.5-K Liquid Supply	4.5-K Liquid Storage	4.5-K Vapor Return	12-K Supply and Return	63-K Supply and Return
Pressure, atm	1.0	1.0	0.0164	18	18
Diameter, cm	7.6	7.6	30.5	4.8	15.2
Length, m	250	350	250	500	500
Friction pressure drop	0.029 psi	0.30 psi[b]	0.312 torr	4.8 psi	3.7 psi
Heat load, W	0.291[a]	2.8[a,b]	16.5[a]	6.2	1100
Cost, 10^6	0.52	0.73	1.56	0.43	1.80
Total cost, 10^6					5.04

[a] Includes frictional pumping power.

[b] Includes lateral supply line used for transfer to storage.

D. LOW-PRESSURE PUMPING SYSTEM

A pressure drop of 0.30 torr for the 4.5 K vapor return line from the dewar to the cold box and a 2.0-torr pressure drop in the cold box gives a pump inlet pressure of 10.3 torr. The corresponding pump inlet volume flow is 74 600 ℓ/s (159 000 cfm). The cost of the pump motors is $408 000, and the cost of the pumps is $3.17 million for a total of $3.58 million. The volume of the pumping system is 169 m^3, and the weight is 62 900 kg. These costs are for the cold box and pumping system located below ground at the same level as the coil. The first stage booster pump is a lobe-type positive displacement pump, motor driven with V-belts, and includes a vacuum control and blower exhaust temperature switch. The second stage forepump is an oil-sealed mechanical vacuum pump, motor driven with V-belts.

E. DEWAR HEAT EXCHANGER

The main function of the cryogenic system is to maintain the superconducting energy storage coil at 1.8 K. Besides providing for the heat sinks and shields at intermediate temperatures, the refrigerator must satisfy the 1.44-kW heat-conduction load from the struts, the 0.50-kW radiation, and the 0.3-kW coil losses to the 1-atm 1.8 K bath. A heat exchanger or evaporator, composed of 62 vertical pipes on 6.7-m centers in each of the 13 dewar sections, is manifolded into circumferential headers. The pipes are located between the inner wall of the helium vessel and the inner coil surfaces. The 1.8 K superfluid helium at 12.5 torr in the heat exchanger pipes is supplied by expansion at the dewar of liquid subcooled by heat exchange with the 1.8 K vapor from the dewar to a temperature below 4.5 K. The vertical pipes are filled with 1.8 K superfluid He II, and heat is transported with sonic velocity through the superfluid to the helium-vapor interface at the top of the vertical pipes. There, helium is evaporated into the circumferential headers which are manifolded into the 4.5 K 30-cm-diam vapor return line. The largest He II superfluid temperature rise, 0.03 K, is in the vertical heat exchanger pipes in the center coil dewar segment. All other temperature gradients are at least an order of magnitude less. The heat exchanger cost is estimated to be $1 million.

F. REFRIGERATOR

The refrigerator supplies 162 g/s of liquid helium at 4.5 K and 1 atm for the 1.8 K system. This liquid is expanded through a J-T valve to the 1.8 K and 12.5-torr level into the dewar heat exchanger. In addition, the refrigerator supplies 250 ℓ/h (8.33 g/s) at 4.5 K and 1 atm for cooling the 50-kA electrical leads. The combined 4.5 K load is 4.1 kW. The 12 and 63 K shielding and conduction loads are, respectively, 9.3 and 144 kW. The combined loads from Tables V-I and V-II and those just given are presented with the refrigerator parameters in Table V-III.

G. HELIUM INVENTORY

The helium inventory for the system is 1.4×10^6 m^3 and will cost $1.68 million if purchased as gas.

TABLE V-III

CRYOGENIC REFRIGERATOR SUMMARY

				Totals
Temperature, K	4.5	12.0	63.0	
Total refrigeration loads, kW	4.1	9.3	144	
Ideal refrigeration work ratio, W/W	65.7	24.0	3.76	
Ideal refrigerator input power, kW	269	223	541	
Carnot efficiency fraction	0.25	0.25	0.25	
Actual refrigerator input power, kW	1080	893	2170	4140
Volumes, m^3	464	145	38	647
Weights, kg	102 500	33 700	9 600	145 800
Costs, $\$10^6$	2.64	2.31	4.30	9.25

H. COOLING TOWER

A double-flow wood cooling tower with a 50-hp motor is required. The installed tower would cost $30 000.

I. HELIUM STORAGE

The 2.0×10^6 ℓ of liquid helium in the system will be stored in eight 227 000-ℓ dewars on the surface near the refrigerator compressor station above the equipment room. A pump to transfer the liquid will be located below the coil dewar and will reverse the flow of the fluid through the lateral 4.5 K supply line between the cold box and dewar. The liquid bypasses the cold box and flows to the surface through a vertical transfer line. The storage system parameters and costs are given in Table V-IV.

TABLE V-IV
LIQUID HELIUM STORAGE SYSTEM

Dewars	
Volume, ℓ (gal)	227 000 (60 000)
Quantity	8
Cost, $\$10^6$	3.6
Pump	
Flow rate, g/s	375
Head, m (psi)	225 (40)
Efficiency, %	60
Power, kW	1.39
Cost, $\$10^6$	1.0
Total cost, $\$10^6$	4.6

REFERENCES

1. D. B. Colyer and R. I. Schermer, "1-GWh Diurnal Load-Leveling Superconducting Magnetic Energy Storage System Reference Design; Appendix E: Cryogenic System," Los Alamos Scientific Laboratory report LA-7885-MS, Vol. VI (1979).

2. R. I. Schermer, "1-GWh Diurnal Load-Leveling Superconducting Magnetic Energy Storage System Reference Design; Appendix A: Energy Storage Coil and Superconductor," Los Alamos Scientific Laboratory report LA-7885-MS, Vol. II (1979).

3. J. G. Bennett and F. D. Ju, "1-GWh Diurnal Load-Leveling Superconducting Magnetic Energy Storage System Reference Design; Appendix C: Dewar and Structural Support," Los Alamos Scientific Laboratory report LA-7885-MS, Vol. IV (1979).

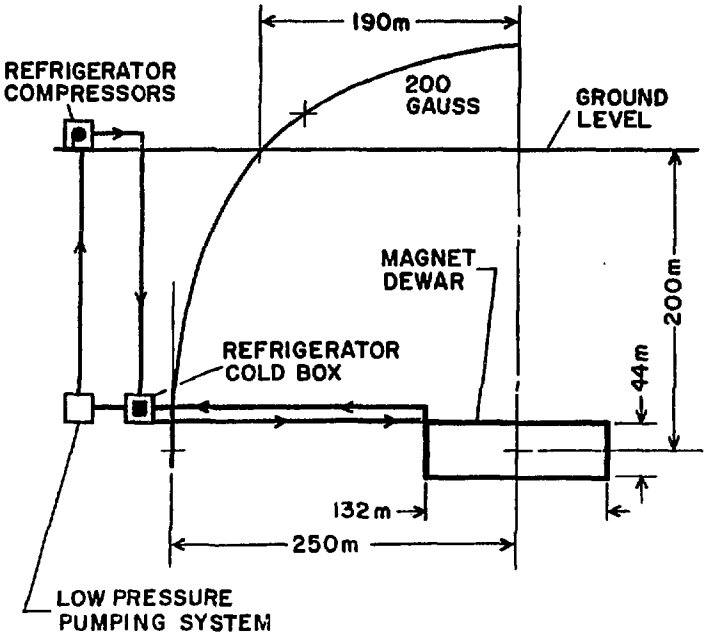

Fig. V-1.
Cryogenic components arrangement.

CHAPTER VI

ELECTRICAL SYSTEM

A. INTRODUCTION

The power conversion equipment forms the interface between the utility bus and the superconducting magnetic energy storage coil. The equipment consists of several parallel-connected converter transformers, each tied to a line-commutated converter. The transformers provide the voltage transformation from the high-voltage level of the utility bus to the medium-voltage level at the converter input. The converter provides bidirectional power flow between the three-phase ac system and the dc coil. The rating of the power conversion equipment requires that it be divided into two identical modules, each of which in turn consists of four identical submodules. The heart of each submodule is a converter transformer and two parallel-connected Graetz bridges forming one 12-pulse bridge. The design of these units is described below, followed by a discussion of reactive-power requirements, filtering, and entire electrical system cost estimate.

The SMES unit should be located as close as possible to the load center to minimize transmission losses between the generators and the load. The transmission losses, because of their quadratic dependence on the current, are the lowest if the energy is transmitted at constant power. With a storage unit close to the load the power can be transmitted from a distant generating station to the load at constant rate, and the transmission line may be designed for average power instead of peak power.

The SMES unit should be interfaced with the lowest voltage system available that can absorb and deliver the real power pulses without endangering the stability of the system and can absorb the voltage fluctuations caused by the reactive-power variations. Low transformer primary voltage guarantees a compact transformer design and makes a series connection of a power and a converter transformer unnecessary. The assumption is made that a 230-kV system with a short-circuit capacity of over 4 000 MVA is adequate to be used for the installation of a 1-GWh 250-MW SMES unit.

By using the experience gained from converter stations for HVDC transmission lines, which also employ line-commutated converters of the type used for SMES units, 12-pulse converter modules are the best choice with respect to the pulse number of the converter. A converter with a lower pulse

number, such as six, would need more filtering because of the higher-harmonic current content. The complexity and additional cost of a higher-pulse-number converter, such as a 24-pulse unit, would overshadow the reduced filter requirement.

Individuals in electric utility companies have mentioned that energy storage systems should be capable of operation at a fixed or constant power level. This appears to be a somewhat arbitrary requirement. The use of a constant voltage or mixed constant-voltage constant-power SMES system, if it is acceptable to the utility industry, makes the converter equipment less expensive. A constant-power converter is presented below, and the cost for a constant voltage converter is also given.

Different circuit configurations suitable for SMES converters are presented in the Appendix F.[1] Based on these circuits, the series-parallel switching scheme as shown in Fig. VI-1 results in the lowest installed converter power and cost for a constant-power system. This circuit configuration results in a 40% reduction in the converter size compared to a converter unit which is designed for maximum voltage and maximum current. The converter center point can be connected to ground in the series-module connected mode. During the parallel connection of the modules, the ground connection has to be switched off. A constant-voltage converter would not require switching and would need less reactive-power compensation.

B. CONVERTER SYSTEM DESIGN

The design requires an energy exchange of 3.6×10^{12} J in 4 h at a constant-power rate with a maximum charging or discharging power of 250 MW. Maximum and minimum current and voltages are, respectively, 50 and 15 kA and 16.7 and 5.0 kV. Figure VI-2 shows the voltage, current, and power relationship for the SMES system in per unit and absolute parameter values. A line-commutated converter with silicon controlled rectifiers (SCRs) as switching elements is uniquely qualified as the power conditioning equipment for a SMES unit. Two converter modules with a 25-kA current rating and a 10-kV voltage rating at 12.5 kA are required to guarantee 250-MW output power under all load currents. The area bordered by dashed lines in Fig. VI-2 represents the operating range of the two converter modules. A voltage drop of 1.0 kV at 25 kA results in a module rating of 11 kV and 25 kA. The total installed converter power is 2 × 11 kV × 25 kA = 550 MW. If two 8.33-kV 25-kA converter

modules are used and a 10% voltage increase of the no-load voltage over the rated voltage is allowed, then the installed converter power is reduced to 2 × 9.16 kV × 25 kA = 458 MW. However, the converter would not be capable of providing 250 MW in the current range of 25 to 28.8 kA. The darkened area in Fig. VI-2 indicates the insufficient converter power for this case. At 25 kA, the maximum power would be 218.6 MW instead of 250 MW. The smaller converter rating is justified in spite of the 12.6% reduction in output power within a small current range because of the substantial saving of 92 MW of converter power. At 40 $/kW, this results in a saving of $3.68 million.

The constant-power rating of 250 MW over the full current range requires an installed converter power of 458 MW. If the mixed mode of operation would be acceptable with a constant-voltage operation at 8.33 kV up to 30 kA and a constant-power operation at 250 MW between 30 and 50 kA then the installed converter power could be 406 MW. Equations (F-15) and (F-16)[1] give the lower installed capacity for the module by-pass switching scheme with two converter modules. The total installed converter power has been reduced by 52 MW; but, in addition, the mixed mode of operation allows the use of the module by-pass switching scheme at a lower per unit cost of $35/kW.

C. CONVERTER MODULE DESIGN

Each of the two converter modules for the constant power circuit has a rating of 9.16 kV and 25 kA. The design of a converter module with a rating of 229 MW requires dividing the module into several submodules. Based on experience gained from operation of HVDC converters with series-connected SCRs and high-current power supplies with parallel-connected SCRs, the module is subdivided into four 12-pulse submodules, each with a rating of 2.29 kV and 25 kA. A 12-pulse submodule consists of two parallel-connected 6-pulse Graetz bridges, each with a rating of 2.29 kV and 12.5 kA. Figure VI-3 shows the circuit diagram of a converter module with the four submodules and the eight 6-pulse Graetz bridges. Three submodules can be by-passed by a switching arrangement, shown as a mechanical switch in Fig. VI-3, to operate as many submodules as needed close to their maximum voltage. This arrangement reduces the reactive-power requirement considerably. The rating of the Graetz bridges determines the rating of the four converter transformers of each module. The phase voltage and phase current of the secondary transformer winding are 0.97 kV and 10.21 kA, respectively; and the transformer rating for one 6-pulse

bridge is 29.7 MVA. The converter transformers have two secondary windings, one connected in wye and one in delta to the two Graetz bridges of a submodule. The transformer rating of the primary side is 3% less than the sum of the transformer secondary side rating because the primary transformer phase currents are more sinusoidal. The total converter transformer rating is 60 MVA. The parallel connection of the two Graetz bridges requires an interphase reactor to provide current sharing of the two bridges. The rating of the interphase reactor should be 6.125 kA and 1.2 kV.

D. GRAETZ BRIDGE DESIGN

The rating of the Graetz bridge is 2.29 kV and 12.5 kA. The maximum voltage stress of the SCRs is equal to the peak value of the converter transformer secondary line-to-line voltage, 2.37 kV. To stand voltage transients a safety factor of at least two is used so that the SCRs should be designed for 4.7 kV. With present technology, for instance, for the Westinghouse Electric Corp. TA 20 series, 67-mm cells, three series-connected 2000-V SCRs are adequate to provide the voltage rating. A water-cooled Graetz bridge, with an inlet water flow rate of 3 gpm and one SCR of the TA 20-14 type in each leg, can carry a dc current of 4.7 kA. A 10% loss in the current-carrying capability of parallel-connected devices requires a 12.5-kA bridge to have four SCRs in parallel. In total, one 28.62-MW Graetz bridge is equipped with $6 \times 3 \times 4 = 72$ SCRs. A 229-MW converter module consists of $8 \times 72 = 576$ SCRs, and the total 458-MW converter is equipped with $2 \times 576 = 1152$ SCRs. Table VI-I summarizes the parameters for the converter and its subelements.

E. REACTIVE-POWER REQUIREMENT

Line-commutated converters, working in both the rectifier and the inverter mode of operation, require reactive power. Equipment has to be installed to compensate for the reactive-power demand of a SMES unit and to improve the power factor. Different VAR generators such as switched capacitors, overexcited synchronous condensers, and static VAR generators with controlled inductance can be used as reactive-power compensation equipment. Fast-switching load-tap changers are another possibility for reducing the reactive-power demand. However, a recent study by General Electric (GE)[2] on this topic has revealed that this option is not cost competitive. The static

TABLE VI-I

CONVERTER PARAMETERS[a]

Converter module	
Maximum current	25 kA
Load voltage at 25 kA	8.33 kV
No-load voltage	9.16 kV
Power rating	229 MW
Number of converter modules	2
Number of submodules in a converter module	4
Submodule	
Maximum current	25 kA
Load voltage at 25 kA	2.08 kV
No-load voltage	2.29 kV
Power rating	57.25 MW
Number of Graetz bridges in a submodule	2
Graetz Bridge	
Maximum current	12.5 kA
No-load voltage	2.29 kV
Power rating	28.63 MW
Number of 2000-V 1400-A, watercooled SCRs, 3 in series, 4 in parallel for each leg of the bridge	72
Submodule Transformer	
High voltage	230 kV
Low voltage	1.68 kV
Secondary phase current	10.21 kA
Power rating	60 MVA

[a]Two converter modules in series-parallel switching arrangement for 250-MW output power.

VAR generator with a controlled inductance has many attractive features, such as low maintenance and fast response. This scheme should be used in conjunction with a SMES system when the SMES unit is used for storage purposes and system stabilization. If the SMES unit is used only for storage, less expensive switching capacitors are adequate for VAR compensation.

As the voltage is reduced to zero at the end of a charging or discharging cycle maximum full-load reactive power is absorbed by the SMES unit. With the coil current at about its maximum value, one 12-pulse submodule is by-passed. Of the remaining three submodules, two are at the maximum voltage, whereas the third submodule operates with a delay angle of 66^{o} to generate a 0.05 per unit output voltage, for a total submodule voltage of 0.3 per unit. If the commutation reactance is neglected and only the displacement reactive power in the one submodule with the 75.5^{o} phase-delay angle is calculated, then the reactive-power requirement is 58.1 MVAR. Commutation reactive power must be added to the displacement reactive power. The maximum commutation reactive power occurs at the maximum current with the lowest driving voltage applied. At this stage of design, without knowing the exact leakage reactances of the transformer primary and secondary winding, the commutation reactive power can only be estimated to be about 50 MVAR. The total reactive power is, therefore, about 100 MVAR. For a converter operated in mixed mode, the reactive power is reduced by 20%.

F. FILTER

Twelve-pulse line-commutated converters generate line-current harmonics with frequencies of $12n \pm 1$ ($n = 1,2,3...$) times the line frequency. The 11-th and 13-th harmonics are the most critical. Narrow-band high-Q filters for these two harmonics have to be supplemented by a broad-band damped filter effective for the 23-rd and higher harmonics. About half of the required reactive power can be supplied by the ac filters with the remainder supplied by the static VAR generator. Figure VI-4 shows the required components for a total SMES system.

G. COST

The converters outlined in this design can be built with present technology. Cost figures for 12-pulse line-commutated converters used in many applications like HVDC lines, reversible dc-motor drives, and power supplies for large magnet systems are available. Based on the power rating, costs from $35 to $60/kW have been quoted in the literature. A good estimate for the 458-MW converter system is $40/kW, which is very close to a cost figure obtained in a recent GE[2] study on SMES converter costs. This number includes the costs for the converter transformers, the Graetz bridges, the by-pass switches, the control, and the filter networks. An additional cost of $25/kVA occurs for the VAR generator. Table VI-II summarizes the cost for the total converter system. The costs are in 1977 dollars; however, if the converter cost development over the last 10 yr is an indication for the future, then the converter cost will stay constant for the next 5 to 10 yr. Advances in SCR technology will increase the SCR sizes and decrease the ratio of price to SCR power. The decrease in SCR prices will compensate for the inflation rate and increased copper prices.

Because of the installed reactive-power control equipment, the performance of the overall system has been improved with respect to voltage fluctuations. The VAR equipment can also be controlled to compensate for reactive loads other than the SMES unit. In addition, the VAR control equipment can be used in the utility system when the storage unit is not functioning.

TABLE VI-II

COST FOR POWER CONDITIONING EQUIPMENT
FOR THE 1-GWh 250-MW SMES UNIT

	Constant Power Mode 458 MW, 50 MVAR		Mixed Mode 406 MW, 40 MVAR	
	Unit Cost $/kVA	Total Cost $10^6	Unit Cost $/kVA	Total Cost $10^6
Converter including transformers SCR bridges, filters, by-pass switches, and building	40	18.3	35	14.2
VAR generator	25	1.3	25	1.2
		19.6		15.4

REFERENCES

1. H. J. Boenig, "1-GWh Diurnal Load-Leveling Superconducting Magnetic Energy Storage System Reference Design; Appendix F: 1-GWh Electrical System Design," Los Alamos Scientific Laboratory report LA-7885-MS, Vol. VII (1979).

2. C. B. Lindh, R. V. Pohl, and H. T. Trojan, "1-GWh Diurnal Load-Leveling Superconducting Magnetic Energy Storage System Reference Design; Appendix G: Design Study: Thyristor Converter Stations for Use with Superconducting Magnetic Energy Storage Systems," Los Alamos Scientific Laboratory report LA-7885-MS, Vol. VIII (1979).

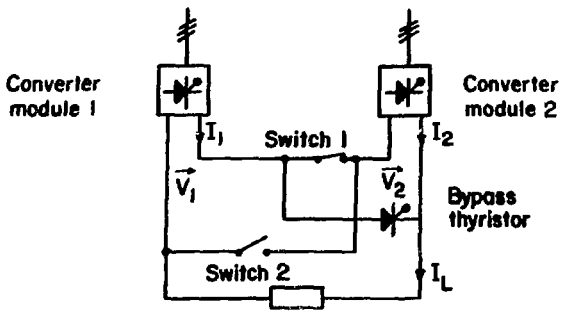

Fig. VI-1.
Series-parallel converter module switching circuit.

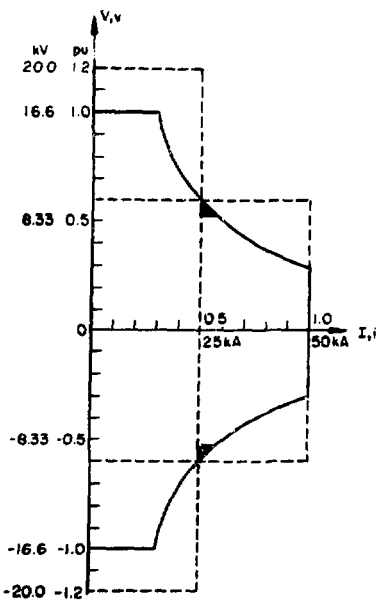

Fig. VI-2.
Current-voltage diagram of SMES unit and converter.

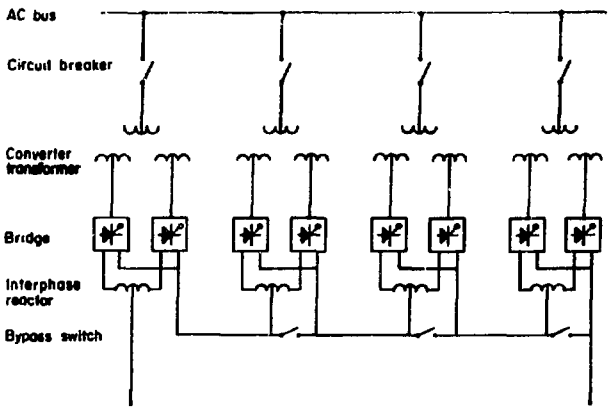

Fig. VI-3.
Power circuit for a module.

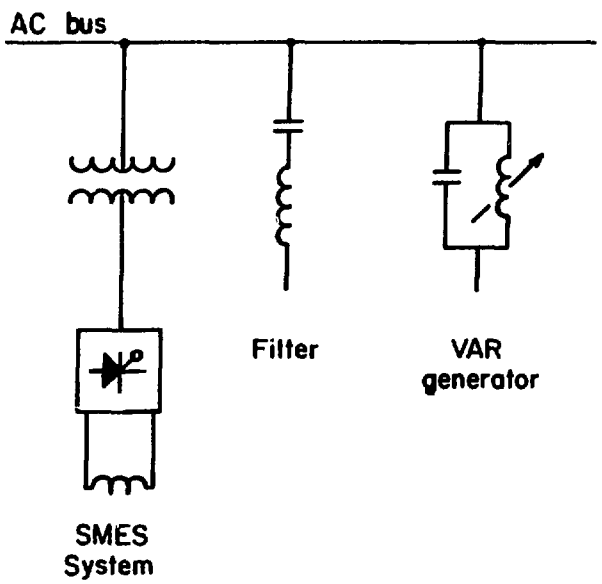

Fig. VI-4.
Overall SMES electrical system.

CHAPTER VII

VACUUM SYSTEM

A. VACUUM VESSEL AND PUMPING SYSTEM

The configuration of the coil cryostat is that of a thin annulus. The dewar has a mean diameter of 132 m and a height of 44 m. The radial thickness has not been determined by any requirements in the preceeding chapters. It is assumed to be 3 m, which is the width of the excavation. This is sufficient to accommodate all of the structure and leave 75 cm of clearance between the wall of the helium vessel and the wall of the vacuum vessel for welding. From these dimensions the volume and surface area are given in Table VII-I.

The dewar is located 200 m below the surface of the earth. Three pairs of diffusion pumps are located at the lower level and are coupled as closely as possible to the dewar wall. They are equally spaced around the lower circumference of the dewar and are connected by appropriately sized lines to a single line that runs to the equipment room and the mechanical blowers and pumps. See Figs. VII-1 and VII-2. The equipment room is 250 m from the vertical center line of the coil to be in a 200 G field for maintenance. One of the major problems in the design of the vacuum system is the impedance of the vacuum lines from the dewar to the equipment room.[1,2] Only the diffusion pumps, right angle valves, and the refrigerated baffles are located immediately adjacent to the dewar. These items will have to be modified for pneumatic or hydraulic control in the magnetic field.

Even though care will be taken during construction to attain and maintain a clean vessel, there still remains a large problem with out-gassing from both the structure and the walls. In the vacuum vessel there will be 960 tonnes of fiber glass reinforced epoxy or polyester struts with a surface area of

TABLE VII-I

DEWAR VOLUME AND SURFACE AREA

	Vacuum Vessel	Helium Vessel
Volume, m3	5.4×10^4	3.8×10^3
Net volume, m^3	5.0×10^4	2.0×10^3
Surface area, m^2	4.0×10^4	3.7×10^4

1.3×10^4 m^2 and 32 tonnes of aluminized Mylar superinsulation. From these two items and the stainless steel and aluminum surfaces, an out-gassing load of 1.6×10^5 torr-liter/s [3,4] can be expected after 1 h of pumping.

If a minimum of six oil diffusion pumps is considered together with matching roughing and foreline pumps as detailed in Table VII-II and Fig. VII-2, then the dewar can be routinely evacuated in 48 h once the initial cleanup of water vapor and organic condensables has been accomplished. Current catalog prices for the materials and main components for the vacuum system are given in Table VII-II. Ideally, cryopanels or cryopumps could be used during cleanup of the system, but this is impossible because of the dewar's location and because of the magnetic fields.

B. LEAK DETECTION

A basic tenet of constructing a vacuum vessel is not to have any inaccessible, untested vacuum joint or seam.[3] Because the dewar is buried, some type of limpet leak testing of all joints and seams will have to be done during construction. It is proposed that testing bells and fixtures be constructed to match contours of the dewar surfaces. These fixtures will have sealing edges of adiprene modified with castor oil for added adhesion. All vessel joints, penetrations, welds, etc, will be x-rayed and leak checked with a helium mass spectrometer as construction progresses.

C. INSTRUMENTATION

Instrumentation will monitor pressure at strategic points on the vacuum vessel, the pressure at inlets to diffusion pumps, and the inlet temperatures of the mechanical blowers and the roughing pumps. Thermocouples will monitor the temperature of the refrigerated baffles at the diffusion pumps and the temperatures of the mechanical blowers and the roughing pumps. Electrical position indicators for all remotely operated valves and a gas analyzer to detect the source of vacuum leaks from outside air, liquid-nitrogen system, or liquid-helium system will be installed. Electrical interlock circuits will be used to protect both the dewar and components of the pumping system. Current prices for instrumentation are shown in Table VII-III.

TABLE VII-II

VACUUM SYSTEM COMPONENTS AND COSTS

Item	Quantity	Unit Cost, $	Total Cost, $
32-in. diffusion pump	6	9 000	54 000
Diffusion pump control	6	620	3 720
32-in. refrigerated baffle	6	7 330	46 980
32-in. right-angle valve	6	9 600	57 600
Valve position indicator	10	121	1 210
36- by 36- by 30-in. Tee	3	6 050	18 150
16-in. Tee	3	1 285	3 855
16-in. slide valve	6	2 816	16 896
8-in. slide valve	12	905	10 860
16- by 8-in. cross	6	1 765	10 590
16- by 12-in. cross	3	1 901	5 703
12-in. slide valve	6	1 100	6 600
Mechanical blowers	6	11 730	70 380
8-in. Ell	6	270	1 620
8- by 8- by 4-in. Tee	24	620	14 880
8-in. cross	6	679	4 074
8- by 4-in. reducing Ell	6	175	1 050
Piston pump	18	9 850	177 300
26-in. pipe (1000 ft)	1	140 640	140 640
16-in. pipe (500 ft)	1	27 500	27 500
8-in. pipe (300 ft)	1	4 200	4 200
Expansion joint	2	1 159	2 318
26-in. expansion joint	2	1 229	2 458
		Total	682 584

D. OPERATION

Under normal operation, the vacuum system will be pumped from atmospheric pressure to hard vacuum under manual control. Electrical interlock circuits will ensure proper sequencing and operation of the vacuum system. If a fault or malfunction occurs, an alarm monitoring the affected parameter will sound and automatic action taken to shut down equipment to protect the rest of the

TABLE VII-III

INSTRUMENTATION (3 REQ'D)

Item	Quantity	Unit Cost, $	Total Cost, $
Hot filament ionization	22	755	16 610
Gauge with thermocouple cable (1230 ft)	4	3 075	12 300
Cable (10 ft)	18	50	900
Residual gas analyzer	1	8 885	8 885
Leak detector	1	8 600	8 600
Sequential valve controller	2	1 566	3 132
	Total per station		50 427
	Total		151 281

system. Pairs of diffusion pumps will be manifolded together so that if a malfunction occurs, equipment fails, or need for maintenance arises, equipment can be isolated from the system and redundant equipment can be brought on line. Routine operation will be controlled by a microprocessor or minicomputer with fault condition and parameter status displayed.

REFERENCES

1. S. Dushman and J. M. Lafferty, Scientific Foundations of Vacuum Technique (John Wiley and Sons, Inc., New York, 1962, Second Edition).

2. M. Pirani and J. Yarwood, Principles of Vacuum Engineering (Reinhold Publishing Corporation, New York, 1961).

3. L. Holland, W. Steckmacher, and J. Yarwood, Vacuum Manual (E. and F. N. Spon, London, 1974).

4. N. L. M. Demis and L. A. Heppell, Vacuum System Design (Chapman and Hall Ltd., London, 1968).

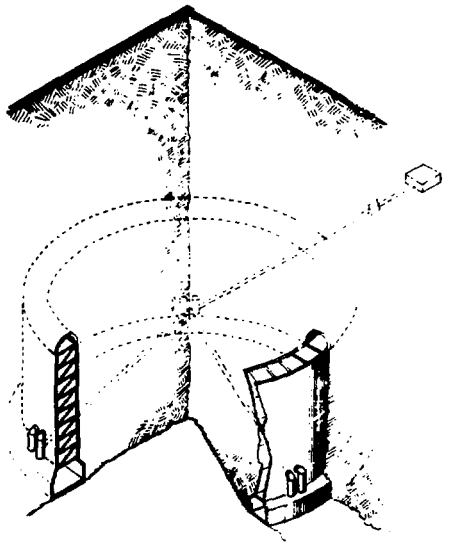

Fig. VII-1.
Dewar and vacuum system.

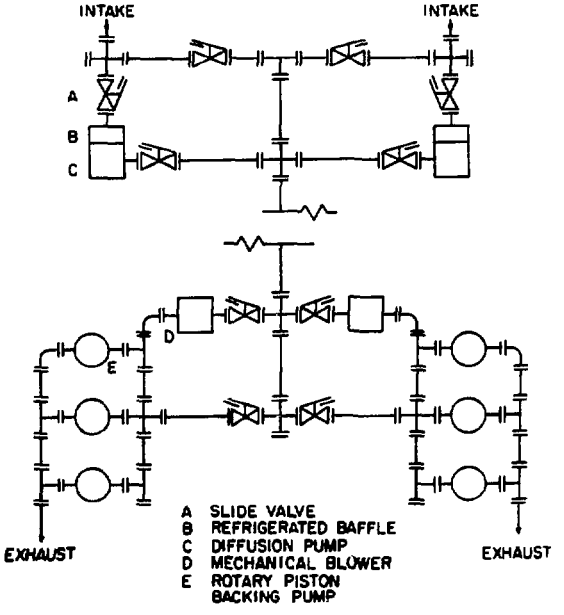

Fig. VII-2.
Piping schematic for vacuum system.

CHAPTER VIII
GUARD COIL

A. INTRODUCTION

The effect of the constraints on the magnetic field beyond the fence around the 1-GWh SMES coil on the land requirements and a possible guard coil are examined in this chapter. If the property line can be at a field of 10^{-3} T or more an economical guard coil will have little effect on the location of the boundary. A guard coil can reduce the land requirement by at least a factor of 4 if the property line is at a field of 3×10^{-5} T. A guard coil located at the same depth as the main storage coil is more effective than a guard coil at ground level; but neither has much effect on the field at ground level directly over the main coil. This field can only be controlled by locating the main coil deeper. A conceptual design and cost estimate is presented for a typical guard coil.

B. GEOMETRICAL CONSIDERATIONS

As indicated in Fig. VIII-1, a point in space may be specified in either cylindrical coordinates, R and Z, or in spherical coordinates, r and θ, where the coordinate origin in each case is taken at the midplane on the storage coil solenoid axis. The relation between the two coordinate sets is

$$r^2 = R^2 + Z^2 \qquad \text{(VIII-1)}$$

and

$$\tan \theta = R/Z \quad .$$

The magnetic field at any point for a solenoid will have two orthogonal components. It is most convenient to take these as the cylindrical components, B_R and B_Z, expressed as functions of r and θ. For distances large enough such that

$$r^2 > a^2 + (b/2)^2 \quad ,$$

where a and b were defined in Chapter II, the magnetic field may be expanded in terms of an infinite series in odd powers of 1/r, the leading terms of which are

$$B_Z = \frac{3\mu_o NIa^2}{4\ r^3}\ (\cos^2\theta - \frac{1}{3}) \qquad \text{(VIII-2a)}$$

and

$$B_R = \frac{3\mu_o NIa^2}{8\ r^3}\ \sin 2\theta \quad . \qquad \text{(VIII-2b)}$$

The leading terms represent the field to within a few percent for r > 5a.

Suppose that a second or guard coil, energized in a sense opposite to the main coil, is placed so that its midplane and axis, and thus its coordinate origin, is coincident with the origin of the main coil. The quantity NIa^2 appearing in Eqs. (VIII-2a) and (VIII-2b) is called the dipole moment of the coil. Clearly, if the dipole moment of the guard coil is equal and opposite to that of the main coil, the field at large distances from both coils will be greatly reduced. This result, which will be referred to as a shield with a matched dipole moment, provides only an approximate design basis for the guard coil. The detailed design will depend on the exact nature of the environmental restrictions ultimately placed upon SMES. Because these restrictions are not defined at present, this chapter illustrates how various possible sets of constraints can be met. This can sometimes be accomplished with a guard coil that will be a good deal simpler and less expensive than the matched dipole.

Designing for a matched dipole moment does provide a qualitative guide for reducing the cost of the guard coil. The cost of all the guard-coil components will increase with the coil-winding volume, which is proportional to the conductor length. A matched dipole moment is expressed by the equation

$$(NI)_g = \frac{NIa^2}{(a_g)^2}, \qquad \text{(VIII-3)}$$

where the subscript g denotes the guard coil. The length of the guard-coil winding, $2\pi a_g N_g$, decreases as $1/a_g$. A large diameter guard coil will thus be less expensive than a small diameter coil. The guard coil can have a very different cross section from that of the main coil. It might, for instance, be a loop of circular cross section with major radius $a_g >> a$. A simple loop of appropriate size exhibits too large a field at the conductor surface; however, the cost of conductor decreases with decreasing magnetic field. Thus, a solenoid with height several times the radial thickness is more economical. Because the guard coil cost must be a modest fraction of the main coil cost, $a_g >> a$. Such a guard coil will have very little effect upon the total field in the region $R \leq a_g$.

C. ECONOMIC AND ENVIRONMENTAL CONSTRAINTS

A general class of environmental constraints will define the magnetic field at and beyond a given boundary, with access inside the boundary limited to plant employees. The appropriate action to satisfy these constraints will be qualitatively different based upon the value of the field and the boundary specified. The following representative field values, which elicit very different actions, are used as a basis for guard coil design.

1. 2×10^{-2} T (200 G). This is the standard for extended exposure of the whole body as set by the directors of the Stanford Linear Accelerator Center (SLAC) in 1970 and is the most conservative of all similar standards.
2. 10^{-3} T (10 G). This is less than the value of 12 G, which is reported to activate certain types of cardiac pacemakers.
3. 3×10^{-5} T (0.3 G), which is the average value of the earth's field.

A great difference in guard-coil design will exist if these field limitations apply to different accessible regions, such as

1. everywhere at and above ground level, $Z \geq 200$ m and $R \geq 0$,
2. at and above ground level but beyond some boundary, $Z \geq 200$ m and $R \geq R_b$, or
3. above some height and beyond some boundary $Z \geq Z_b \geq 200$ m and $R \geq R_b$.

If any of the three field conditions must be met for the region defined under 1, the guard-coil design will be more critical than if the same field condition applies to regions defined by 2 or 3. Combining the three-field and

three-space requirements results in nine different sets of environmental constraints. Whichever constraints apply must be met at minimum cost, with the guard coil and the land required for the facility being the only significant capital costs.

To limit the field beyond the fence line at ground level, the easiest and least expensive solution is to buy enough land if it is available. Table VIII-I gives the radius and area requirements needed to meet field constraints 1, 2, and 3 for various depths below the earth's surface of the midplane of the 1-GWh storage coil. Here, as in all cases in this chapter, numerical results were obtained by computer calculation. In some cases the amounts of land indicated in Table VIII-I will simply not be obtainable.

Locating the coil deeper might lead one to think that a positive effect would result, but Table VIII-I reveals the limited utility of this strategy. The reasons are clear from Eqs. (VIII-1) and (VIII-2). Close to the coil axis, $r \approx z$, and the high fields close to the coil are sensitive to the coil depth. However, very low field values occur where $R >> Z$ and $\theta \to 90^{\circ}$. Further, as the storage coil is located deeper below the surface, the value of B_R at ground level increases as θ decreases. The net effect is that $\bar{B}$ will change direction rapidly but will decrease only very slowly in magnitude for very large changes

TABLE VIII-I

RADIUS AND AREA REQUIRED TO ATTAIN

VARIOUS FIELDS AT GROUND LEVEL

Midplane Coil Depth, m	Field, T	R, m	Area, $(km)^2$
200	2×10^{-2}	200	0.13
	1×10^{-3}	650	1.3
	3×10^{-5}	2140	14.4
400	2×10^{-2}	0	0
	1×10^{-3}	620	1.2
	3×10^{-5}	2140	14.4
600	1×10^{-3}	500	0.79
	3×10^{-5}	2130	14.3
800	1×10^{-3}	200	0.13
	3×10^{-5}	2100	13.9
1000	1×10^{-3}	0	0
	3×10^{-5}	2080	13.6

in coil depth. Similarly, the field above ground level at large R decreases slowly with height above ground level. This fact is clearly shown in graphs of the field from the main coil presented in Fig. VIII-2.

The incremental cost of changing the main SMES coil depth is $3 million per 100 m according to Appendix D.[1]

The above discussion brings out the qualitative difference which environmental restrictions will make. If the field everywhere above ground were restricted to less than 200 G, the problem could be solved without a guard coil by locating the storage coil deeper, although this response would be useless if the 0.3-G criterion were to apply.

D. SOLUTIONS FOR VARIOUS FIELD CONSTRAINTS

The constraint combinations whose solutions are easily treated are presented below.

1. Field at Ground Level Less Than a Specified Value for All R

To hold the field to a quite low value at all points at ground level is the most severe restriction because of the great difficulty in reducing the field directly above the main coil. Locating the storage coil deeper and deeper is required as the acceptable field is decreased. Table VIII-II gives the on-axis field at ground level as a function of the depth of the coil midplane for an unshielded coil. The depth becomes unreasonable at some field level on the order of 5×10^{-4} T. To be effective in this region of space, a guard coil would have about the same radius as the main coil and, from previous arguments, would be about as expensive. The guard coil would have to be well separated from the main storage coil, so as not to affect the stored energy, and yet would have to be located fairly deeply so that Eq. (VIII-2) applies everywhere above ground.

In summary, the field everywhere above ground level may be economically reduced below 2×10^{-2} T but probably not below 10^{-3} T by simply burying the magnet. Still lower field restrictions will be very expensive to meet. At present there is no reason to suspect that an extremely low field will be required directly above the coil.

2. Field Limited to Less Than 2×10^{-2} T Inside a Radius for All Z and Above a Fixed Height for All R

The 2×10^{-2} T point occurs close enough to the storage coil so that a guard coil is relatively ineffective in determining its location. The same holds roughly for the 10^{-3} T point. Table VIII-I shows that the land area requirement to meet the criterion is very modest, and Table VIII-II shows that an axial separation of 302 m is required. Thus, the maximum field that would be produced at heights more than 100 m above ground level by a coil located 200 m below ground is 2×10^{-2} T. As above, more restrictive conditions directly above the storage coil can only be treated by locating the coil deeper, compensated by an even smaller ground-area requirement.

In addition, the field gradient at the 2×10^{-2} T point is very small. For a storage coil located 200 m below the ground, the gradient at the surface would be of the order of 2×10^{-4} T/m, directed downward and inward. The estimated force on a piece of iron in this environment is 4% of its weight, which is too small to create a safety hazard.

3. Boundary Field Is Limited to a Value Between 10^{-3} And 3×10^{-5} T

These cases involve the detailed design of a guard coil. The guard coil also greatly reduces the field above ground at locations beyond the guard-coil radius. As above, however, there is little that can be done other than locating the storage coil deeper to reduce the field directly above the main coil.

TABLE VIII-II

FIELD AT GROUND LEVEL, ON-AXIS,
AS A FUNCTION OF STORAGE COIL DEPTH

Field, T	Depth, m
6.39×10^{-2}	200
2×10^{-2}	302
$2 \times 10-3$	660
1×10^{-3}	833
3×10^{-4}	1250
3×10^{-5}	2690

E. GROUND LEVEL VERSUS BURIED SHIELDS

The storage coil located 200 m below ground level has 2.14×10^8 A-turns at a mean radius of 66 m. Consider a guard coil designed in keeping with Eq. (VIII-3) with radius a_g = 330 m, which requires that $(NI)_g = 8.6 \times 10^6$ A-turns. This guard coil must also be located at 200 m below ground level. The field distribution from the coil pair is shown in Fig. VIII-2. At ground level, the field will be reduced below 3×10^{-5} T at R = 1050 m, an improvement over R = 2140 m for the unshielded coil. The corresponding values for 10^{-3} T and 2×10^{-2} T are 510 and 170 m, respectively.

This equal moment criterion gives neither the best design nor is it the only option available. For instance, if the guard coil is designed to cancel exactly B_Z at ground level and R = 850 m, then $(NI)_g = -7.82 \times 10^6$ A-turns, which is 9% less conductor than for the guard coil based on the matched dipole criterion. The field distribution from this guard-coil main-coil pair, as shown in Fig. VIII-2, is much more complex than that from the matched dipole, and the field at very large distances is larger. The 3×10^{-5} T point, however, is moved in to R = 910 m, and the R values for 10^{-3} and 2×10^{-2} T are virtually unchanged. Thus there is an economically optimum guard coil that is less expensive than the matched dipole guard coil, but its characteristics will depend on the exact environmental constraints.

Whereas the cost of the guard coil can be estimated, underground installation costs are less well known. If the coil could be wound in a roughly finished circular cross-sectional area cavern with a 3-m diam and an excavation cost of $\$100/m^3$, the tunnel cost would be \$1.5 million. If a larger or better finished tunnel is required, the cost will increase accordingly.

The possibility of locating the guard coil at ground level remains. The primary fact about such a coil is that it can affect only the Z component of the field at ground level. Thus, the fence line can only be moved in to the point where B_R alone has decreased below the allowed value. For reference, a guard coil has been chosen at ground level with a_g = 330 m and $(NI)_g = -5.50 \times 10^6$ A-turns that exactly cancels B_Z at R = 850 m. Field profiles for this guard-coil main-coil pair are shown in Fig. VIII-3. The fence line for 10^{-3} T is at 610 m, with R = 1620 m for $8 = 3 \times 10^{-5}$ T. The 3×10^{-5} T fence line could be moved inward to R = 1550 m at the expense of moving the 10^{-3} T point outward and building a guard coil with significantly more ampere turns, approaching a matched dipole moment.

Locating the storage coil deeper is counter-productive. Because only B_Z can be canceled with a ground-level guard coil, the net field will actually increase and the fence line will move outward for either 10^{-3} T or 3×10^{-5} T. Again, restrictions at R = 0 that necessitate locating the main coil deeper, create a difficult situation. A significant reduction in B_R at ground level can be obtained, however, with a guard coil located closer to the surface than to the main storage coil.

F. REFERENCE GUARD COIL DESIGN

The parameters of the reference guard coil are presented in Table VIII-III. The same 50-kA conductor as in the main storage coil is used with an overall current density of 5×10^7 A/m^2, which allows room for spacers and structure. A loop of circular cross section would have a surface field of 5.9 T, rather larger than is desirable. The rectangular configuration is 5 turns thick radially, 22 turns high axially, and has a maximum field of 5.0 T.

TABLE VIII-III
GUARD COIL PARAMETERS

Z_g, vertical location	ground level
a_g, mean radius, m	330
b_g, height, m	0.574
c_g, radial thickness, m	0.191
N_g, number of turns	110
ℓ_g, conductor length, m	2.30×10^5
I_g, maximum current, kA	50
B, maximum field, T	4.9
L_g, self inductance, H	39
M, mutual inductance to main coil, H	7.6
ΔW, MWh	+8.3
T_o, operating temperature, K	1.85
Vacuum vessel minor diam, m	1.0

The forces can be calculated accurately by treating the guard coil as though the cross section were circular. The magnetic force on the guard coil may be broken into three contributions. The first, caused by the axial and radial fields of the main storage coil, is outward and upward. The second arises from the large poloidal field of the conductors, which acts to decrease the winding cross-sectional area. The resulting pressure is approximately 10^7 MPa (1400 psi) and is well below the stress limit of the conductor. Because the guard coil has the form of a large loop, the third contribution, which is the axial field due to other parts of the guard coil, produces an outward force. The fields at the guard coil at maximum charge are $B_R = 6.9 \times 10^{-3}$ T and $B_Z = -1.56 \times 10^{-2}$ T. The guard coil itself contributes -1.47×10^{-2} T to B_Z. The resulting force components are given by

$$\bar{F} = NI\bar{B} \quad , \qquad \text{(VIII-4)}$$

$$F_Z = 3.78 \times 10^4 \text{ N/m upward} \quad ,$$

and

$$F_R = 8.58 \times 10^4 \text{ N/m outward} \quad .$$

The upward force should be compared to a conductor weight of 1.73×10^3 N/M.

It is possible to consider warm support for the coil. The required strut cross-sectional area for a compressive strength of 280 MPa (40 ksi) is only 0.7 m^2, and the strut cost and strut heat leak are both trivial compared with those for the storage coil. There is, however, a geometric problem. The dewar cost, a major expense item, is very sensitive to the minor radius. It would then be necessary to design struts which are multiply re-entrant to have a long thermal path but a short overall physical length. An alternative is to provide cold support. The vector sum of F_Z and F_R can be supported in hoop tension by 0.11 m^2 of alloy aluminum at a stress of 280 MPa (40 ksi) and a material cost of \$1.76/kg. The upward force must be transmitted to the outer vessel wall by means of fiber glass straps set into long, re-entrant tubes in the outer wall. The upward force can be balanced by several meters of earth. For cost purposes

the weight of the concrete foundation is equal to this levitating force. A total of 3330 m^3 of concrete is required, at an installed cost of \$500/m^3. With cold support, the heat leak into the guard coil is very small compared to the main storage coil. Thus, the refrigeration requirement and the helium inventory have been neglected.

Component costs of the guard coil are given in Table VIII-IV, where the same cost factors have been used as in Appendices A[2] and C[3]. The superconductor is not graded, and the dewar is constructed of 0.5-cm-thick aluminum alloy. A vacuum vessel 1.0 m in cross-sectional diameter leaves more than enough space for insulation and for construction tolerances.

G. SHIELD CURRENT, VOLTAGE, AND ENERGY

As seen in Table VIII-III, the self-inductance and mutual inductance of the guard coil are both considerably less than the self-inductance, L = 3170 H, of the main storage coil. The effective inductance of the two opposed coils is given by $L' = L + L_g - 2M$. The fractional effect on energy storage is

$$\frac{\Delta W}{W} = \frac{L'-L}{L} = \frac{L_g - 2M}{L} \quad . \tag{VIII-5}$$

Table VIII-III gives ΔW.

TABLE VIII-IV

COMPONENT COSTS FOR GUARD COIL

Item	Cost, $10^6
50-kA superconducting cable	7.8
Stabilizer, fabricated	1.9
Coil winding labor	1.5
Structural support	3.3
Dewar	1.5
Concrete foundations	1.7
Total	17.7

During discharge the main coil current swings from +50 to +15 kA; and the guard-coil current must swing from -50 to -15 kA. If the guard coil is in the persistent mode,

$$M \frac{dI}{dt} + L_g \frac{dI_g}{dt} = 0$$

and

$$\Delta I_g = -\frac{M}{L_g} \Delta I = -0.195\ \Delta I = +\ 6.82\ \text{kA} \quad . \qquad \text{(VIII-6)}$$

This change in I_g is such that the field of the main coil at +15 kA and the guard coil at -43.18 kA is less than or equal to the field, at all points, when both coils are operating at full current. Thus, it is sufficient to operate the guard coil in the persistent mode to eliminate the heat leak from the high-current leads.

To charge the guard coil from an external power supply in 4 h takes 136 V. The actual design would probably have more turns of conductor and would operate at lower current and higher voltage.

REFERENCES

1. "1-GWh Diurnal Load-Leveling Superconducting Magnetic Energy Storage System Reference Design; Appendix D: Superconducting Magnetic Energy Storage Cavern Construction Methods and Costs," prepared by Fenix and Scisson, Inc., Tulsa, OK, Los Alamos Scientific Laboratory report LA-7885-MS, Vol. V (1979).

2. R. I. Schermer, "1-GWh Diurnal Load-Leveling Superconducting Magnetic Energy Storage Reference Design; Appendix A: Energy Storage Coil and Superconductor," Los Alamos Scientific Laboratory report LA-7885-MS, Vol. II (1979).

3. J. G. Bennett and F. D. Ju, "1-GWh Diurnal Load-Leveling Superconducting Magnetic Energy Storage System Reference Design; Appendix C: Dewar and Structural Support," Los Alamos Scientific Laboratory report LA-7885-MS, Vol. IV (1979).

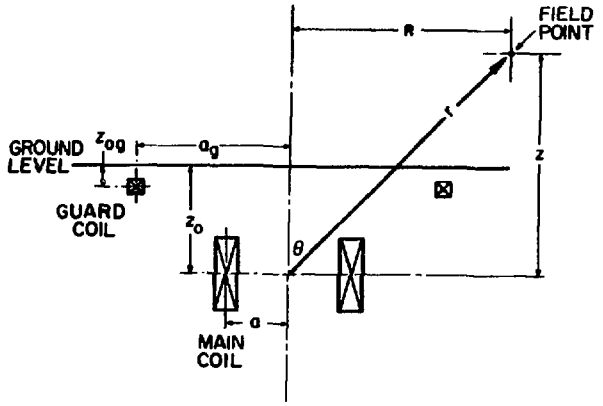

Fig. VIII-1.
Geometric variables for guard coil calculations.

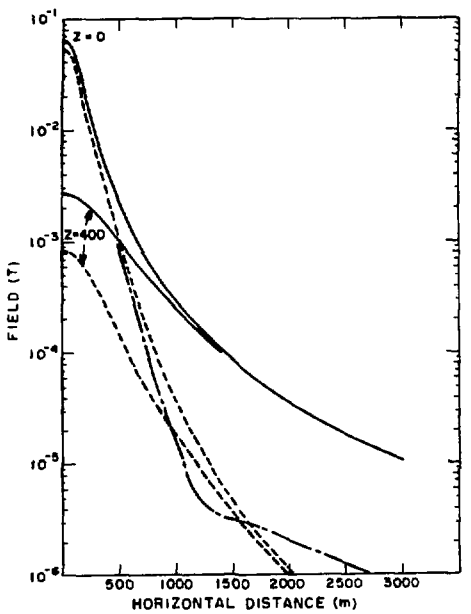

Fig. VIII-2.
Magnetic field as a function of horizontal distance from coil axis at ground level (Z=200) and 400 m above ground (Z=600 m). Guard coil buried at same depth as main coil. Solid curves - main coil only; dashed curves - storage coil plus guard coil with matched dipole moment; dotted curve - storage coil plus guard coil chosen to make B_Z = 0 at ground level and R = 850 m.

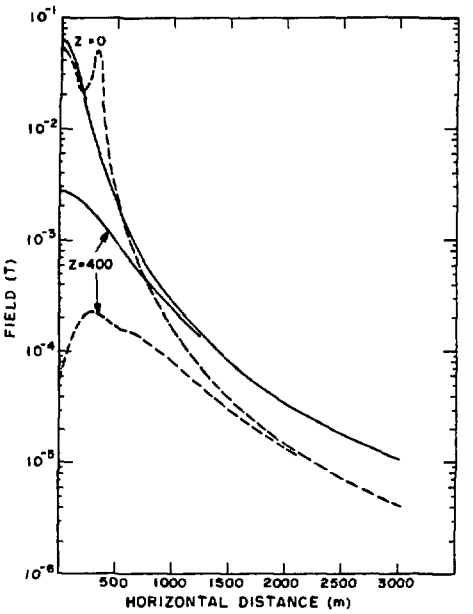

Fig. VIII-3.
Magnetic field as a function of horizontal distance from coil axis at ground level (Z=200) and 400 m above ground (Z=600 m). Solid curves - main coil; dashed curves - storage coil plus guard coil at ground level chosen to make B_Z = 0 at R = 850 m.

CHAPTER IX
COSTS

The costs provided in previous chapters are not on a common basis because of their diverse origins and because different contributors were involved with the designs for each chapter. This chapter compiles the costs and adds profit, installation costs, and engineering design costs for those items and facilities where they have not already been incorporated. Engineering includes complete design and specification for manufacture, fabrication, field operations, installation, and construction; architectural services; and project management of the SMES system. When profits, installation, and engineering design costs are not listed in Table IX-I, they are already included in the base number. For all items additional cost detail can be found in the appropriate chapters and appendices. All costs are in current dollars except as noted. No land costs are included.

The principal costs for the system occur in five areas. These areas are the coil and conductor, the dewar and structural support, the cavern or excavation, the cryogenic system, and the electrical system. The costs represent current technology and are for a base reference design. Materials selection has been for those requiring the least development, such as a built-up welded stainless steel dewar. Costs are based upon information obtained on recent purchases, contracts, major installations, and studies conducted for this reference design. In some instances the sources of cost data are confidential and the amounts must be taken at face value. Engineering costs not originally included in the base numbers are added at 15%.

A discussion of the large cost items follows. From this, certain indications of possible reductions are developed and a lower cost list is presented in Table IX-II.

The single largest cost for the conductor and coil at $72.9 million is the 50-kA, graded superconducting cable at $43.2 million. This amount is based on present costs of NbTi superconductor for projects such as the energy-doubler magnets for the Fermi National Accelerator Laboratory and the Brookhaven accelerators. The prospect of reducing this cost by a factor of 2 in a large scale operation is credible. The superconducting cable cost included in the $51.3 million for conductor and coil in Table IX-II is $21.6 million. The

TABLE IX-I

COST OF 1-GWh SMES UNIT

	10^6
Conductor and coil	72.90
Profit on aluminum matrix	0.57
Engineering at 15%	11.02
Winding machine	3.50
Dewar and structural support	90.56
Engineering at 15%	13.58
Cavern	33.80
Cryogenic system	
Transfer lines	5.04[a]
Valves	2.00[a,b]
Low-pressure (12.5-torr) pumping system	3.58[a]
1.8 K heat exchanger	1.00
Cooling tower	0.03
Helium storage dewars	3.60
Liquid helium storage pumps	1.00
Refrigerator	9.25[a]
Installation[a]	5.96
Engineering[a]	2.98
Helium gas	1.68
Electrical system	15.40[c]
Vacuum system	0.83
Installation	0.83
Engineering at 15%	0.25
Guard coil	17.70
Engineering at 15%	2.66
Total	299.72
	$300/kWh

[a]Installation and engineering are included for these items at 30 and 15%, respectively, of their cost. Similar costs for the other items of the cryogenic system are included in their base costs as given.

[b]Valve costs are given at a lower cost than that recommended in Ref. 1 because the long transfer lines will require a proportionally lower relative percentage of valves than used in more conventional systems.

[c]This item is often assigned as a cost to power instead of energy.

TABLE IX-II

REVISED COST OF 1-GWh SMES UNIT

	10^6
Conductor and coil	51.30
Profit for aluminum matrix	0.57
Engineering at 15%	7.78
Winding machine	3.50
Dewar and structural support	42.49
Engineering at 15%	6.37
Cavern	30.00
Cryogenic system	
Transfer lines	5.04[a]
Valves	2.00[a,b]
Low-pressure (12.5-torr) pumping system	3.58[a]
1.8 K heat exchanger	1.00
Cooling tower	0.03
Helium storage dewars	3.60
Liquid helium storage pumps	1.00
Refrigerator	9.25[a]
Installation[a]	5.96
Engineering[a]	2.98
Helium gas	1.68
Electrical system	15.40[c]
Vacuum system	0.83
Installation	0.83
Engineering at 15%	0.25
Guard coil	10.40
Engineering at 15%	1.56
Total	207.40
	$207/kWh

[a]Installation and engineering are included for these items at 30 and 15%, respectively, of their cost. Similar costs for the other items of the cryogenic system are included in their base costs as given.

[b]Valve costs are given at a lower cost than that recommended in Ref. 1 because the long transfer lines will require a proportionally lower relative percentage of valves than used in more conventional systems.

[c]This item is often assigned as a cost to power instead of energy.

major cost saving of using aluminum stabilizer is already shown in Table IX-I. No other significant cost reduction is anticipated in this item.

The dewar and structural support costs listed in Table IX-I are for a stainless steel dewar and G10CR epoxy fiber glass structural supports. The fabricated-shape materials cost of \$4 880/m^3 (\$0.80/lb) for aluminum is from an uninflated 1977 price list[2] and of \$17 300/m^3 (\$1.00/lb) for A304-LN stainless steel is from a Lawrence Livermore Laboratory bid quotation for the Mirror Fusion Test Facility. The cost of G10CR currently ranges from \$6 to \$17/kg. This design study uses \$8/kg in Table IX-I. In addition, a multiplier of 3, applied to the fabricated shape materials costs, was used to estimate the installed costs for the dewar and structural support.

The revised costs of Table IX-II incorporate several considered changes. These are a change from a stainless steel dewar to aluminum, a support structure material cost of \$4/kg based on quantity production and the possible use of a multiplier of 2 for the installed cost of polyester-fiber glass composite and other materials. This last is optimistic. The change from stainless steel to an aluminum dewar requires a change from a 13-segment to a 25-segment dewar. This occurs because the thermal stress is exceeded for an aluminum dewar with fewer segments.

The cavern costs are fixed mostly by the materials and mining equipment. If the rate of excavation is doubled without additional labor and equipment, then a saving of about \$3.8 million can be made.

The cryogenic system cost is an area where engineering optimization would be most productive. The cost was somewhat higher than expected; however, often neglected ancillary items are included. Transfer line costs are based on estimates made available by Cryenco. The refrigerator cost, the installation cost, and the engineering cost are based upon a reasonable extrapolation of large liquid helium plants presently being installed in the U. S. Optimization would possibly reduce the cryogenic system cost by 15 to 30%; however, there would be a compensating increase in the structural support cost for a lower overall net saving. Such an optimization is discussed below but is not included in Table IX-II.

The guard coil cost has been reduced by changes in both the superconductor and dewar costs corresponding to those made above for the main energy storage coil.

Thus, based upon the point reference design and on the material and fabrication costs presented in this report, the capital cost of storing energy in a 1-GWh SMES system ranges from $207 to $300/kWh. These values extrapolate inversely as the maximum energy to the one-third power. For a 10-GWh SMES unit the corresponding costs become $96 and $139/kWh. Clearly, the economy of size is important.

Refrigerator optimization is a rather comprehensive interchange of costs related to whether the cold box is located above or below ground level, length and cross-sectional area of the structural supports, amount of excavation required if the structural supports are made longer, number and temperature level of heat sinks located on the structural supports, dewar radiation shielding, the use of a 1.8 K helium bath instead of a 4.5 K bath, magnetic field, transfer line size, and other system features. Without presenting an extensive optimization, a quick qualitative insight can be gained by merely considering structural supports with reduced thermal conductivity, when the heat leak is reduced by one-half. No other affect is considered. Thus, the nature of the change is phenomenological, and other related costs, such as the support and excavation costs, remain constant. The new refrigerator costs corresponding to the last line of Table V-III become $2.00, 1.42, 2.86, and 6.28 million. The total saving in refrigerator cost is $2.96 million or 32%. Most of the cryogenic components directly related to the refrigerator would be reduced similarly in cost.

The possibility of this type of saving being made without an associated increase for some other part of the system is unlikely. A more realistic percentage reduction by optimization has been judged to be nearer to 20%, although even this appears high for optimization of the entire system. On this basis the unit installed costs for a 10-GWh system would then range from $77 to $111/kWh. These costs are higher by factors of 2 to 3 than previously developed numbers.

REFERENCES

1. D. B. Colyer and R. I. Schermer, "1-GWh Diurnal Load-Leveling Superconducting Magnetic Energy Storage System Reference Design; Appendix E: Cryogenic System," Los Alamos Scientific Laboratory report LA-7885-MS, Vol. VI (1979).

2. Mater. J., Materials Selector 84, No. 6, 26 (1977).

CHAPTER X

DISCUSSION, SUMMARY, AND RECOMMENDATIONS

A. EFFICIENCY

The efficiency of a SMES system is the one unique feature that sets it apart from all other storage systems. This feature is because the stored energy is electromagnetic and does not require conversion to or from either mechanical or chemical states. Converter efficiency is estimated to be 96 ± 1%. For the 1-GWh SMES reference design system the overall efficiency is then calculated to be 83%, which is a combination of electrical and thermal losses.

The refrigerator system considered uses low-pressure pumps and is taken to have an efficiency of 25% of Carnot. This efficiency is identical with those expected for large helium recovery plants now being installed in the US. Refrigerator efficiency can be improved to 30% of Carnot at an estimated 20% increase in refrigerator cost.

If a refrigerator system can be developed with a subcooler cycle instead of using the low-pressure pumps, then the overall efficiency can be improved. Eighty percent of the low-pressure pumping power is estimated to be saved by the subcooler cycle. For a 1-GWh SMES system with a 96% efficient converter, the overall efficiency with the improved refrigerator becomes 86%. If the structural support heat leak is reduced by one-half, the respective overall SMES efficiencies are 89 and 91%.

Size is an important factor affecting efficiency. As the total storage energy changes the thermal losses are approximately proportional to the total outward force on the coil or to the surface area of the SMES coil dewar. Thus, losses are proportional to the two-thirds power of the maximum energy stored, which in turn is proportional to the volume of the storage coil. The converter efficiency is the same, 96%, independent of size. For a 10-GWh SMES system, the extrapolated overall efficiencies become 89.8 and 91.3%, respectively, for the system with the more conventional refrigerator with low-pressure pumps and with the subcooler cycle refrigerator. If the structural support heat leak is halved, the respective efficiencies are 92.9 and 93.6%. Clearly size is important not only to cost but also to efficiency.

B. COMMENT

This reference design has examined the major component subsystems of a SMES system. These subsystems are the energy storage coil and conductor, the dewar and structural support, the underground excavation, the cryogenic system, the electrical converter system, the vacuum system, and the guard coil. The foregoing chapters treat the subsystems and their cost. In addition, supplemental volumes to this report, which are included as appendices, elaborate on the extensive technical studies undertaken.[1] These volumes do not themselves include all of the details investigated for the reference design. Some alternative approaches are developed in detail; others, which were generally explored in depth before being abandoned, are merely mentioned. Still others, such as the wire-rope superconducting cable, are relatively new concepts and warrant experimental development. This volume is a condensation and overview of the appendices. Some detailed information is included here as warranted on the topics not covered extensively in the appendices.

C. COSTS

This study is based on a 1-GWh diurnal load-leveling SMES system. This size was chosen to examine the cost of a system, which, if economically competitive, would have a larger market in the utility industry. The cost of the 1-GWh unit was estimated to range from $207 to $300/kWh, which is not economically competitive. For a 10-GWh system these costs scale to $96 to $139/kWh. Optimization might reduce these somewhat further. The lower cost for the 10-GWh unit borders on an economically competitive installed cost for energy storage systems. Earlier studies[2,3] on SMES systems have considerably lower estimated costs in practically every area.

Some of the costs of this design are based on studies contracted with industry with experience in mining, high-purity aluminum production, and manufacture of large converters. Other costs are based on similar types of large equipment currently being installed in the US. Still other costs were based on recent quotations and industrial surveys of the market for fabricated metal shapes. The sources for our cost data are broad based and have considerable expertise contributing to their origins. Thus the costs given here are relevant because of their comparability, and they should be meaningful. Despite this contention and because of the wide range of cost per kilowatt-hour obtained even by this reference design, we recommend that

comprehensive analysis be made to evaluate the cost basis of the two principal SMES reference designs of this study and of Ref. 2.

D. GENERAL PROGRAM DEVELOPMENT

Some aspects are inadequately treated in this design and in previous designs. These include maintenance, reliability, fault-mode analysis, site selection and evaluation, and efficiency. These may or may not influence the costs substantially. For example, design of the vacuum vessels for maintenance could be kept simple if space suit technology can be adapted to function in the cold vacuum space. Thus, a recommendation for the next phase of work is to identify the areas not adequately considered and to fold them into an engineered design, which leads to three related recommendations. The first is to reach a basic conclusion whether large SMES is economically competitive as determined from the analysis and evaluation of the divergent costs estimated by this and other studies. The second, if the conclusion of the first is positive, is to conduct a contracted industrial engineering design study and technology assessment for a 10- to 30-MWh prototype SMES unit. The third is to establish a development program to remedy identified technology deficiencies.

The recommended industrial engineering design study should be less effort than that for a Title I architectural design but sufficiently advanced to make an accurate cost estimate, identify all major engineering problems, assist in identification of all technology deficiencies, and guide the subsequent Title I work. Except to improve upon some peripheral details in very limited areas, the present SMES teams are not equipped to proceed with the 10- to 30-MWh prototype system without the expertise that is available from an industrial construction design firm.

E. CONCLUSIONS

A SMES system has the potential of providing a very advanced and efficient energy storage system for electric utility diurnal load-leveling. The cost of constructing such a system may be high. Nevertheless a more thorough engineering design is warranted. SMES efficiency has been reevaluated in a utility operation simulation in a recent study by Arthur D. Little, Inc.[4] Comparison with battery storage, underground pumped hydrostorage, compressed air energy storage, and conventional generation capacity shows that SMES is economically competitive and is the most attractive of the large systems when

the rated energy delivered per year per unit power capacity is above about 1750 kWh/yr per kW. See Figs. 3.8 and 3.9 of Ref. 4. This result is predicated upon system costs a factor of about 2 to 3 lower than those developed here and efficiencies of at least 90%.

REFERENCES

1. "1-GWh Diurnal Load-Leveling Superconducting Magnetic Energy Storage System Reference Design; Appendices A through G," Los Alamos Scientific Laboratory report LA-7885 MS, Vols. II through VIII (1979).

2. R. W. Boom, Ed., "Wisconsin Superconductive Energy Storage Project," Vols. I and II, Engineering Experiment Station, College of Engineering, University of Wisconsin report (1974 and 1976).

3. W. V. Hassenzahl, B. L. Baker, and W. E. Keller, "The Economics of Superconducting Magnetic Energy Storage Systems for Load Leveling," Los Alamos Scientific Laboratory report LA-5377-MS (August 1973).

4. "An Evaluation of Superconducting Magnetic Energy Storage," Arthur D. Little, Inc., report, to be published.

☆ U.S. Government Printing Office: 1979 — 677—115/218